Matthias A. Blatnik

The σ-Meson in the Bethe-Salpeter Approach

Diplomarbeit

zur Erlangung des akademischen Grades eines
Magisters
an der Naturwissenschaftlichen Fakultät der
Karl-Franzens-Universität Graz

Betreuer:
Univ. Prof. Dr.
Reinhard Alkofer

Institut für Physik, Fachbereich Theoretische Physik

2012

Matthias A. Blatnik

The σ-Meson in the Bethe-Salpeter Approach

Diploma thesis

to obtain the scientific degree
Magister
at the Faculty of Natural Sciences,
University of Graz

Advisor:
Univ. Prof. Dr.
Reinhard Alkofer

Department of Physics, Theory Division

2012

Contents

Für Ludmilla, Maria und Erich
aber vorallem für Sebastian
-
to my grandparents
who showed me that success can only be accomplished through hard work

Chapter 1

Introduction

1.1 The Strong Interaction and the Symmetries of Quantum Chromodynamics

During the last thirty to forty years the description of the strong interaction via the theory of Quantum Chromodynamics (QCD) has been generally accepted. Being a renormalizable, non-abelian gauge Quantum Field Theory it is based on the invariance under local $SU(3)$ transformations in color space [1, 2, 3, 4, 5]. The mediating gauge bosons are the so-called gluons A^a_μ which carry a color index a and a Lorentz index μ. They transform according to the adjoint representation of $SU_C(3)$. The other fields involved are the quarks, represented by Grassmanian fields q^f_α, and the Grassmanian ghosts c^a which are introduced in the so-called "Faddeev - Popov - method"[6, 7]. However the appearance of ghosts is due to the mentioned specific gauge fixing procedure and choosing a specific gauge, i.e. Landau gauge. Moreover the ghosts do not couple directly to quarks they can be separated from the related parts in the partition function $Z[J, \bar{\eta}, \eta]$ (c.f. Sec. 1.2).
The quarks in contrast to the gluons belong to the fundamental representation of the mentioned color group and carry also a second index which is called "flavor" $f = 1, \ldots, N_f$. The current belief is we have three generations of quarks, namely *up* and *down*, *strange* and *charm*, *bottom* and *top*, already ordered recording to their mass. With this three fundamental entities as input the classical action of QCD reads

$$S[\bar{q}, q, A_\mu] = \int d^4x \, \mathscr{L}_{\mathrm{QCD}} \tag{1.1}$$

whereas the Lagrangian density of QCD can be written as follows

$$\mathscr{L}_{\mathrm{QCD}} = \mathscr{L}_{\mathrm{YM}} + \mathscr{L}_{GF} + \mathscr{L}_{\mathrm{quarks}}. \tag{1.2}$$

The ghost fields $(\bar{c}^a, c^a)$ appear only in the gauge-fixing term of the Lagrangian $\mathscr{L}_{GF}$ and only couple directly to the Yang-Mills [8] sector. But as we tend to model this part in the further scope of this work it is possible to neglect the ghosts contribution from this point on. Applying all simplification to Eq. (1.2) and presenting two additional definitions, the covariant derivative $D_{\mu;\,\alpha\beta}$ and the field strength tensor of the gluon field $F_{\mu\nu}$ that stem from the analogy with Quantum Electrodynamics (QED) the QCD Lagrangian becomes

$$\mathscr{L}_{\mathrm{QCD}} = \sum_{f=1}^{N_f} \sum_{\alpha,\beta=1}^{3} Z_2 \bar{q}_\alpha^f \left(i \not{D}_{\alpha\beta} - Z_m \, m_0^f \, \delta_{\alpha\beta} \right) q_\beta^f - \frac{1}{2} \operatorname{tr}(F_{\mu\nu} F_{\mu\nu}) + \mathscr{L}_{GF} \tag{1.3}$$

with

$$D_{\mu;\alpha\beta} = \delta_{\alpha\beta}\partial_\mu - ig(t^A)_{\alpha\beta} A_\mu^A$$

and

$$F_{\mu\nu} = \partial_\mu A_\nu - \partial_\nu A_\mu - ig[A_\mu^{(B)}, A_\nu^{(C)}]$$

where the abbreviation $A_\mu = A_\mu^A t^A$ is used and $^{(B),(C)}$ account for different color indices than $_{-}^{A}$. The t^A's are the hermitian generators of the color group $SU(3)$. In the fundamental representation these generators t^A are proportional to the Gell-Mann-matrices $\lambda^A = 2t^A$ and fulfill the following normalization condition and commutator relation

$$\operatorname{tr}\left(\frac{\lambda^A}{2} \frac{\lambda^B}{2} \right) = \frac{1}{2}\delta^{AB}, \qquad \left[\frac{\lambda^A}{2}, \frac{\lambda^B}{2} \right] = i f^{ABC} \frac{\lambda^C}{2}. \tag{1.4}$$

The f^{ABC} are called *structure constants* of the corresponding Lie algebra $\mathfrak{su}(3)$ and generate the adjoint representation of the color group $SU(3)$.
As can easily be seen the Lagrangian density $\mathscr{L}_{\mathrm{QCD}}$ fulfills conservation laws with respect to parity and charge conjugation and if the current quark mass(es) m_0^f is/are set to zero the QCD-Lagrangian is also invariant under a global transformation with respect to the flavor degree of freedom. These transformations are of the form

$$q_i \longrightarrow (U_V)_{ij} q_j = e^{i\theta_V^A \left(\frac{\lambda^A}{2}\right)_{ij}} q_j, \tag{1.5}$$

$$q_i \longrightarrow (U_A)_{ij} q_j = e^{i\gamma_5 \theta_A^A \left(\frac{\lambda^A}{2}\right)_{ij}} q_j. \tag{1.6}$$

Both equations build up together the so-called "chiral transformations" whereas (1.5) is called a "vector -" and (1.6) a "axial-vector transformation". With the use of γ_5 - matrices, still being in the limit of vanishing quark masses, it is possible to divide the interactions between the quarks into left-handed and right-handed quark fields q_L & q_R:

$$q_R = \frac{1}{2}(1+\gamma_5)q\,, \qquad \bar{q}_R = \frac{1}{2}\bar{q}(1-\gamma_5), \tag{1.7}$$

$$q_L = \frac{1}{2}(1-\gamma_5)q\,, \qquad \bar{q}_L = \frac{1}{2}\bar{q}(1+\gamma_5). \tag{1.8}$$

Expressing the quark field q and the anti-quark field $\bar{q}$ through q_L and q_R in $\mathscr{L}_{\mathrm{QCD}}$ and using the properties of γ_5, $\{\gamma_5, \gamma_\mu\} = 0$ and $\gamma_5^2 = 1$, it is straightforward to see that the term in (1.2) concerning the quarks splits into two independent parts. The left-handed and right-handed fields are fully decoupled hence

$$\bar{q}\gamma_\mu q = \bar{q}_R\gamma_\mu q_R + \bar{q}_L\gamma_\mu q_L.$$

Each of these terms is again invariant under a unitary transformation of the kind of Eq.(1.5) with new phase angles θ_R and θ_L

$$q_R \longrightarrow U_V(\theta_R)q_R, \tag{1.9}$$
$$q_L \longrightarrow U_V(\theta_L)q_L. \tag{1.10}$$

The associated symmetry group of the Lagrangian (1.2) in the chiral limit can be broken into semi-simple groups

$$U_R(N_f) \times U_L(N_f) \cong U_{L+R}(1) \times U_{L-R}(1) \times SU_L(N_f) \times SU_R(N_f). \tag{1.11}$$

The first term on the right-hand side is linked via Noether's theorem to the baryon number current $J_\mu^B \sim \bar{q}_i(x)\gamma_\mu q_i(x)$ which is conserved exactly in nature. As usual, when dealing with Noether's theorem the conserved current stems from an invariance of the theory, in this case the invariance under a global phase shift for both left- and right-handed quarks. The symmetry $U_{L-R}(1)$ on the other side is not apparent in the hadronic spectrum and therefore must be broken. How this is done is subject to studies of the so-called $U_A(1)$-anomaly but is not part of this work. Nevertheless it has been the subject of several studies (e.g. [9, 10, 11] or [12]).
The remaining symmetry group $SU_L(N_f) \times SU_R(N_f)$ is called *chiral symmetry*. It is broken spontaneously, so that the hadronic vacuum is only invariant under one of the $SU(N_f)$ subgroups, and later also explicitly due to the quark masses. In the case of the spontaneous symmetry breaking Goldstone's theorem predicts $N_f - 1$ massless Goldstone bosons with negative parity. When dealing only with light-flavored quarks (namely *up* and *down*) with masses of some MeV ($m_{\mathrm{up}} \approx 1.7 - 3.3$ MeV, $m_{\mathrm{down}} \approx 4.1 - 5.8$ MeV [2]) the $SU_L(N_f = 2) \times SU_R(N_f = 2)$ chiral symmetry is approximately conserved and the Goldstone bosons require a small mass because of the explicit breaking due to the light quark masses of u/d. The lightest pseudo-scalar isotriplett of particles (namely the pions π^+, π^0, π^-) which carry a considerably smaller amount of mass than other mesons can be identified with these obtained Goldstone bosons.
Including the strange-quark ($m_{\mathrm{strange}} = 101^{+29}_{-21}$ MeV [2]) in the discussion eight Goldstone bosons should be obtained. Nevertheless as the strange-quark mass is of the order of the fundamental scale of QCD $\Lambda_{\mathrm{QCD}} \sim 200$ MeV chiral symmetry is no longer well conserved as in the two-flavor case. It is possible to identify the pions π, the kaons K and the η as the related eight Goldstone bosons. The mesons including a strange quark (K's and η) have

a slightly higher mass due to the "more" explicit symmetry breaking of the s-quark mass m_{strange}.
We disregard the remaining three quark flavors as their current masses are considerably higher and their effect on low-energy processes can be neglected.

1.2 Non-perturbative Methods – from Green's Functions to Dyson-Schwinger Equations

On Green's functions:
In the next few lines we want to introduce some theoretical concepts needed throughout this work concerning Green's functions, functional methods, Dyson-Schwinger equations, etc. The classical action and the Lagrangian of QCD were already given in detail in Eq. (1.1) and (1.2). Evaluating the corresponding equations of motion using the Lagrangian would give a sophisticated way in classical mechanics to extract information. Nevertheless in quantum theories formulated via the Feynman path integral [13] and Schwinger's functional approach [14, 15] new approaches are needed. One of these is the Dyson-Schwinger approach where the "quantum" equations of motion of the Green's functions are provided. It is a quantum field theoretical, non-perturbative approach in the continuum, dealing with the evaluation of an infinite tower of the, before mentioned, Green's functions and relations between them. DSEs also have been shown to be successfully applicable in hadron phenomenology via the combination with the framework of Bethe-Salpeter equations for quark–anti-quark bound states.
To start from a point concerning Green's functions we proceed as follows. The n-point connected Green's functions are defined as the time-ordered vacuum expectation value of n Heisenberg creation or annihilation operators:

$$G^{(n)}\left[\Phi_1 \dots \Phi_n\right] := \langle \Omega | T[\phi_1 \dots \phi_n] | \Omega \rangle \tag{1.12}$$

$$\sim \prod_{i=1}^{n} G^{(2)}_{0;i}\, S[\Phi_1 \dots \Phi_n]. \tag{1.13}$$

Thereby the last line is a formal form of the so-called LSZ reduction formula [3, 16] where $\sim$ was used to indicate an equivalence of the pole structure on both sides. It indicates the connection of an n-point Green's function with the S-Matrix of n-particle scattering.

On Dyson's approach to Green's functions:
F. Dyson has developed two sets of equations in his papers 1949 about the S-matrix in QED [17, 18] which are called Dyson equations. As well as LSZ they are also a manifestation of the strong relation of Green's functions with the S-matrix. While Dyson has given only two equations for the 2-point- and the 3-point-function the principle can straightforwardly be

generalized to the case of n-particle Green's functions. This can be done by summing up all n-particle irreducible interactions in terms of Feynman diagrams. Following first Feynman's theory expanding in orders of the structure constant α, one draws all Feynman diagrams contributing to the interaction of a certain process up to order α, sum them up and extract finally observable quantities like the differential cross-section valid up to the order in α. Following the example of renormalizability, i.e. if a theory is renormalizable to all orders in perturbation theory (PT) it is assumed to be renormalizable non-perturbatively, the Dyson resummation is also valid in the non-perturbative regime. Following Dyson's approach, as presented in [19], it is possible to write n-particle Green's functions as self-consistent equations including either the T-matrix [20] or proper n-particle irreducible Green's functions. The latter is present in the second equation, (1.15), obtained through the introduction of the n-particle interaction kernel $K^{(n)}$ which is shown in (1.16) to be a sum over all proper k-particle irreducible interactions $K_{\text{irr}}^{(k)}$:

$$G^{(n)} = G_0^{(n)} + G_0^{(n)} T^{(n)} G_0^{(n)}, \tag{1.14}$$

$$G^{(n)} = G_0^{(n)} + G_0^{(n)} K^{(n)} G^{(n)}, \tag{1.15}$$

whereas $K^{(n)}$ is given by

$$K^{(n)} = K_{\text{irr}}^{(n)} + \sum_i K_{\text{irr}}^{(n-1)} \otimes G_{0;i}^{(2)} + \dots \ . \tag{1.16}$$

It is easy to construct the equation showing an infinite sum of terms summed up to be the n-particle Green's function $G^{(n)}$ (shown below). Nevertheless this Dyson equation in spite of being calculable up to any order n is still a perturbative equation since only finitely many of all possible interactions are included. This is straightforward to see if the expression for $K^{(n)}$, given in (1.16), is inserted into the equation below

$$\begin{aligned} G^{(n)} = G_0^{(n)} + G_0^{(n)} K^{(n)} G_0^{(n)} + G_0^{(n)} K^{(n)} G_0^{(n)} K^{(n)} G_0^{(n)} + \\ + G_0^{(n)} K^{(n)} G_0^{(n)} K^{(n)} G_0^{(n)} K^{(n)} G_0^{(n)} + \dots \ . \end{aligned} \tag{1.17}$$

On the Feynman path integral formalism and functional methods:
Having dealt with a classical theory up to this point it is necessary to introduce quantization in order to obtain a quantum theory. This can be done via the method of canonical quantization where for every field present in the theory a canonical momentum is needed to arrive at canonical commutator relations. In this work however we would like to stick to another approach called the *Feynman path-integral approach*. It allows both non-perturbative and perturbative calculations and is already heavily used in lattice QCD (see e.g. [21]) and Dyson-Schwinger studies (e.g. [22]). The approach is based on a functional integral over all possible field configurations including all information about the theory. Examining this functional integral it has been shown, [4], to be similar to a partition function of classical

statistical mechanics. Also it is possible to derive all Green's functions of the theory from it (see Eq. (1.18) and (1.20) or [4]). Therefore the functional integral, written down in Eq. (1.18), can also be seen as a "*Generating functional*" $Z[J]$ which depends only on the sources J of the fields involved. Several mentioned properties are summed up in the following two equations[1]:

$$\begin{aligned} Z[J_i] &\propto \langle\, 0, \infty \,|\, 0, -\infty \,\rangle^{J_i}, \\ Z[J_i] &= \int \mathscr{D}\Phi \, e^{-S[\Phi] + \int \widetilde{d^4x}\, J_i \Phi_i} = \langle e^{J_i \Phi_i} \rangle = \sum_{n=0}^{\infty} G_{i_1 \dots i_n} \, J_{i_1} \dots J_{i_n}. \end{aligned} \tag{1.18}$$

Herein the term $\int \widetilde{d^4x}\, J_i \Phi_i$ is an abbreviation for a four-dimensional space-time integral and possible sums over discrete (Lorentz, Dirac, flavor, color, ...) indices given by the expression: $\sum_a \int \widetilde{d^4x}\, J_{i;a}(x) \Phi_{i;a}(x)$ whereas a is a general index that subsumes the mentioned discrete symmetries. Introduced by J. Schwinger[14, 15] it is a supervector over all contributing sources corresponding to fields in the action S.
In the case of QCD Eq. (1.18) becomes the following integral equation (again modelling the Yang-Mills sector and thus neglecting gauge fixing contributions):

$$Z[j^a_\mu, \bar{\eta}, \eta] = \int \mathscr{D}(A^{\mu;a}, \psi, \bar{\psi}) \, e^{-S[A^{\mu;a}, \psi, \bar{\psi}] + \int \widetilde{d^4x} \left[j^a_\mu(x) A^{\mu;a}(x) + \bar{\eta}(x)\psi(x) + \bar{\psi}(x)\eta(x) \right]} \tag{1.19}$$

with $A^{\mu;a}$ being bosonic fields representing the gluons and ψ and $\bar{\psi}$ are the fermionic fields of quarks and anti-quarks, respectively.
Unfortunately also the path-integral method has some problems, e.g. concerning its mathematical existence in continuous space-time or the sometimes emerging, to the numerically needed Wick rotation related, difficulties appearing with singularities. Nevertheless the action based formalism with the connection to the classical Euler-Lagrange equations culminating in the quantum field theoretical framework of Dyson-Schwinger equations shows analogies to statistical physics.
As mentioned it is sufficient for the definition of a Quantum Field Theory to write down the generating functional. The Green's functions of the theory can now be obtained as functional derivatives with respect to the sources J_i and finally taking the sources to be zero

$$G^{\text{full}}_n[\Phi_1 \dots \Phi_n] = \frac{1}{i^n} \frac{\delta}{\delta J_1} \, \dots \, \frac{\delta}{\delta J_n} \, Z[J_i] \bigg|_{J=0}. \tag{1.20}$$

Via the linked cluster theorem[4], the irreducible (connected) contributions to $G^{\text{full}}_n[\Phi_1 \dots \Phi_n]$ can be extracted. It is simply necessary to subtract all partitionings of n-points giving rise to disconnected contributions given by products of m-point functions ($m < n$). The generating functional for the irreducible (connected) Green's functions is then given by the

[1] We will work in Euclidean spacetime throughout this work which is obtained by a Wick rotation in the time component [23] (see therefore the appendix).

expression

$$W_{\text{conn}}[J] := \ln\{Z[J]\} = \ln\left\{\int \mathscr{D}\Phi e^{-S[\Phi]+\int \widetilde{d^4x}\, J_i(x)\Phi_i(x)}\right\}, \tag{1.21}$$

and the connected n-point Green's functions are extracted through a Taylor expansion of this functional

$$\phi_n^{\text{conn}}[x_1 \dots x_n] = \frac{1}{i^n}\frac{\delta^n W_{\text{conn}}[J]}{\delta J(x_1)\dots\delta J(x_n)}\bigg|_{J=0}. \tag{1.22}$$

Further the normalizations are given by

$$Z[0] = 1 \quad \text{and} \quad W[0] = 0.$$

The functional derivative of $W_{\text{conn}}[J]$ with respect to the source J_i yields the expectation value of the field Φ which can be seen as a classical field variable Φ_c

$$\Phi_c(x, J) = \frac{\delta}{i\delta J(x)} W_{\text{conn}}[J]. \tag{1.23}$$

This expression will be needed in the following definition of the generating functional for the proper *1-particle irreducible* (1 PI) Green's functions. It is obtained via a functional Legendre transform of $W_{\text{conn}}[J]$ given by

$$i\Gamma[\Phi_c] = W_{\text{conn}}[J] - i\int d^4x\, J_i(x)\Phi_{i;c}(x), \tag{1.24}$$

whereas Eq. (1.23) was inserted. $\Gamma[\Phi_c]$ is called "*effective action*" and generates the 1-PI, or *truncated*, Green's functions.

Leaning on the classical idea of the Euler-Lagrange equations where the action of the theory is assumed to be extremal and thus is invariant under small changes in the field variables, in quantum field theories one assumes the generating functional $Z[J]$ to be invariant under a change in the fields $\Phi(x)$ [24]. This can be written as a condition on the functional integral:

$$\boxed{0 = \int \mathscr{D}[\Phi]\exp\left\{-S[\Phi] + \int J_i\Phi_i\right\}\left(\frac{\delta}{\delta\Phi_k}S[\Phi] - J_k\right) =: \left\langle\left(\frac{\delta}{\delta\Phi_k}S[\Phi] - J_k\right)\right\rangle_{[J]}} \tag{1.25}$$

Eq. (1.25), written for different generating functionals leads to one of the following *master equations* for the infinite tower of *Dyson-Schwinger equations*

$$\boxed{\begin{aligned}
\left(-\frac{\delta S}{\delta\Phi_i}\left[\frac{\delta}{\delta J}\right] + J_i\right) Z[J] &= 0\,; && (1.26)\\
-\frac{\delta S}{\delta\Phi_i}\left[\frac{\delta W}{\delta J} + \frac{\delta}{\delta J}\right] + J_i &= 0\,; && (1.27)\\
\frac{\delta\Gamma[\Phi_c]}{\delta\Phi_i} - \frac{\delta S}{\delta\Phi_i}\left[\Phi_c + \frac{\delta^2 W}{\delta J\delta J}\frac{\delta}{\delta\Phi_c}\right] &= 0\,, && (1.28)
\end{aligned}}$$

for the full Green's functions, the connected Green's functions and the proper Green's functions respectively.

1.3 The σ - ($f_0(500)$) - Particle, associated Theories, Experiments and Scalar Mesons in the DSE–BSE framework

In this section we would like to shed some light on scalar mesons which have the same quantum numbers as the vacuum, i.e. $J^{PC} = 0^{++}$. In particular we want to look at the lightest scalar resonance which is called the $f_0(500)$ in [2]. As scalars share the same quantum numbers as the vacuum they can condense into it and so break the global chiral $U(N_f) \times U(N_f)$ symmetry. The detailed mechanism responsible for breaking chiral symmetry in nature is an ongoing discussion since fifty years and far from being (entirely) understood. In addition also the identification of scalar particles is tricky due to their large decay widths and the opening of several decay channels within a short mass range. Hand in hand with the large decay widths goes an overlap between resonances and the background which hinder of course their easy resolution.
Also scalars are expected to mix considerably with scalar non-$q\bar{q}$-states like tetra-quarks ($q\bar{q}q\bar{q}$), glueballs or meson-meson bound states below 1800 MeV. Technically the mass and width of a resonance in general can be identified by investigating the pole structure of the process amplitude (i.e. T- or S-Matrix), in particular via the position of the nearest pole at an unphysical sheet of the complex energy plane, $(E - i\Gamma/2)$. This is the Breit-Wigner resonance formula. It is necessary to mention that this formula only agrees with the pole position in the case of well-separated, most importantly narrow resonances.
Scalars are produced in various experiments including πN-scattering, $p\bar{p}$-annihilation, mesonic decays (J/ψ, $B-$, $D-$, K), $\gamma\gamma$-formation and radiative ϕ-decays. Through isospin ($I = 0, 1/2, 1, 3/2, 2$) the scalar particles are easily classified into f_0's ($I = 0$), a_0's ($I = 1$) and K_0^*'s ($I = 1/2$). Only the $f_0(500)$ (or σ) and the $K_0^*(1430)$ are well-established today but still far from being totally understood. Theoretically several models using two-body unitarity, analyticity, Lorentz-invariance or chiral and flavor symmetry and techniques like effective chiral field theories (e.g. the linear sigma model) have been investigated in parallel to the experiments.
Having introduced scalar particles in general we turn now in particular to the lightest scalar resonance, i.e. the $f_0(500)$ (σ). Being a scalar with isospin zero, $J^{PC} = 0^{++}$ as the vacuum, the σ has first been introduced in the linear sigma model fifty years ago to explain chiral symmetry breaking within that model. It is therefore often referred as the "Higgs boson" of strong interaction as it is important for chiral symmetry breaking (χSB) and thus for the generation of the proton mass, the η'-mass and the so-called "constituent quark mass".
This description and attempts, starting from a chiral Lagrangian (e.g. the NJL model

[25, 26]), first have required the $f_0(500)$ mass and width to be $M_\sigma \approx 700$ MeV & $\Gamma_\sigma \approx 850$ MeV. However in recent studies the σ was placed around 500 MeV [27]. The Particle Data Group places the mass between 400 and 550 MeV and its width between 400 and 700 MeV [28]. Unfortunately the σ pole is difficult to determine due to its large width, the inconsistency with the model of the Breit-Wigner resonance and the distortion by other resonances like the $f_0(980)$ or the $f_0(1370)$ or by the background required by chiral symmetry. Precision concerning the pole determination in theory was finally obtained in the last two decades since the $f_0(500)$ was formally "resurrected" in 1996 by Törnquist and Roos [29] and culminated in a precise pole position within an uncertainty of less than 20 MeV by I. Caprini, G. Colangelo and H. Leutwyler [27]:

$$M_\sigma = 441^{+16}_{-8}\,\text{MeV}, \quad \Gamma_\sigma = 544^{+18}_{-25}\,\text{MeV}. \tag{1.29}$$

Therein the authors used a partial wave decomposition method due to Roy [30] and found that the position of the σ pole depends only on the following three parameters: the isosinglet S-wave phase shift $\Delta\delta_A(800)$ and the S-wave scattering lengths a_0^0 and a_0^2.
Other authors [31, 32, 33, 34] concern themselves with the nature of the σ, i.e. if it is a conventional $q\bar{q}$ state or some $q\bar{q}q\bar{q}$ [35], a meson-meson bound state or a scalar glueball [36, 37]. In reality the $f_0(500)$ of course can be expected to be a superposition of all the before listed. The determination of the main contributing component is model dependent, still under investigation and left for future investigations to clarify.

As other scalar particles the σ is produced in e.g. πN-scattering or $p\bar{p}$-annihilation and data is in particular obtained from $\pi-\pi$, $K-\bar{K}$, $\eta-\eta$ and 4π systems in S-wave. Analysis of several processes obtained the need of four poles, the σ and three other scalars, in the region from the $\pi-\pi$ threshold to ≈ 1600 MeV. Although data on the $\pi-\pi$ S-wave phase shift $\delta_J^I = \delta_0^0$ was obtained already as early as Grayer [38] in 1974 the missing distinct resonance structure under 900 MeV in $p\bar{p}$-annihilation was somehow controversal. It was nevertheless shown [38, 39] that also the $p\bar{p}$-data is described well with the standard solution for the πN-data which allows the existence of the broad-width σ.

As can be seen in [2, 28] the σ decays strongly into two pions thus demanding the application of non-perturbative methods. In this thesis we consider an iso-scalar $q\bar{q}$ meson to model the σ mentioned above. Within the framework of Dyson-Schwinger & Bethe-Salpeter equations which rest on the Green's functions of the underlying theory, QCD, we will construct the QCD gap equation and quark–anti-quark bound states for the iso-scalar and pseudo-scalar case and use them as an input for further considerations.
As in the DSE–BSE framework decay channels of particles are not dynamically included we construct the particular decay of this iso-scalar quark–anti-quark bound state into $\pi\,\pi$ and further their recombination into this "σ" via the so-called triangle diagram $\Gamma_{\sigma\to\pi\pi}$ and the $\pi\pi$-dressing Π ("diamond correction") respectively. We want to stress at this point that

wherever we mention the σ in the further scope of this work within the DSE–BSE approach we actually mean an iso-scalar $q\bar{q}$ state and not the experimentally observed $f_0(500)$. The properties of the considered state are thus a priori only the ones of an idealized chiral partner of the pion.

The outline of this thesis is the following: Chapter one has been used to introduce the fundamental concepts of Green's functions and their "quantum" equations of motion, the Dyson-Schwinger equations (DSEs), chiral symmetry and its breaking as well as theoretical and experimental facts about the $f_0(500)$. We therefore stuck to standard literature [1, 3, 4, 24] and only tried to introduce the subject and emphasized what will be needed throughout this thesis. Chapter two will deal with one of the most used Green's function, the quark propagator in QCD. As we deal with a tower of an infinite number of equations of course our treatment of this two-point function will meet the necessity of a truncation (see therefore chapter 2.2). In chapter three we will derive the framework of the so-called homogenous Bethe-Salpeter equation (BSE) and apply it to the cases of an iso-scalar and a pseudo-scalar meson. In both chapters we will give some numerical results. In chapter four we will combine the theoretical concepts of the DSEs and the BSE to create the so-called *triangle diagram* which gives the possibility to describe a decaying particle in the DSE - BSE framework. Moreover we will include information on numerical results of the hadronic decay width and the coupling strength. Finally in chapter five we combine two triangle diagrams and two "bosonic propagators" to the *diamond diagram*, which we expect to hold information and corrections on the mass and width of the iso-scalar σ meson considered within the DSE-BSE framework. We conclude at the end of chapter five.

Chapter 2

Solving the Quark Dyson-Schwinger Equation

2.1 The Quark DSE

In this chapter we will discuss the quark propagator Dyson-Schwinger equation and its solution which will be needed as an input to solve the Bethe-Salpeter equation. Starting with the first of equations (1.26) substituting the general Φ_i with the anti-quark field $\bar{q}$ the expression changes to

$$\left(-\frac{\delta S_{\rm QCD}}{\delta\bar{q}(x)}\left[\frac{\delta}{\delta j(x)}\,,\,\frac{\delta}{\delta\eta(x)}\right]+\eta(x)\right)\,Z[j,\eta,\bar{\eta}]\;=\;0, \tag{2.1}$$

which also is writeable as an expectation value:

$$\left(-\frac{\delta S_{\rm QCD}}{\delta\bar{q}(x)}\left[\frac{\delta}{\delta j},\frac{\delta}{\delta\bar{\eta}}\right]+\eta(x)\right)\,Z[j,\bar{\eta},\eta]=\Big\langle\,-\frac{\delta S_{\rm QCD}}{\delta\bar{q}(x)}+\eta(x)\Big\rangle_{[j,\eta,\bar{\eta}]}=0. \tag{2.2}$$

Taking the derivative of Eq. (2.2) with respect to $\frac{\delta}{\delta\eta(y)}$, it is possible to arrive at an expression which will be called the *quark Dyson-Schwinger equation*

$$\begin{aligned}\left\langle\frac{\delta S_{\rm QCD}}{\delta\bar{q}(x)}\bar{q}(y)\right\rangle=\mathbb{1}\delta^4(x-y)=Z_2\,(-\partial\!\!\!/+Z_m m)\langle\,q(x)\,\bar{q}(y)\,\rangle\\ -\,Z_{1F}\,i\,g\int d^4z\,d^4z'\,\delta^4(x-z)\,\delta^4(x-z')\,(\gamma_\mu t^A)\langle\,q(z)\,\bar{q}(y)\,A^A_\mu(z')\,\rangle,\end{aligned} \tag{2.3}$$

where several abbreviations were introduced which are given as follows:

$$S(x-y) := \langle\, q(x)\,\bar{q}(y)\,\rangle = \frac{\delta^2 W[j,\bar{\eta},\eta]}{\delta\eta(y)\delta\bar{\eta}(x)}\bigg|_{\bar{\eta}=\eta=0} = \left[\frac{\delta^2\Gamma[A^A_\mu,\bar{q},q]}{\delta\bar{q}\,\delta q}\right]^{-1} \tag{2.4}$$

$$\langle\, q(z)\,\bar{q}(y)\,A^A_\mu(x)\,\rangle = \frac{\delta^3 W[j,\bar{\eta},\eta]}{\delta\eta(y)\delta\bar{\eta}(z)\delta j^a_\mu(x)}\bigg|_{\bar{\eta}=\eta=0} = \int d^4a\,d^4b\,d^4c\,D^{AB}_{\mu\nu}(x-a)\,S(z-b)\,\frac{\delta^3\Gamma[A^A_\mu,\bar{q},q]}{\delta\bar{q}(c)\,\delta q(b)\delta A^B_\mu(a)}\,S(c-y). \tag{2.5}$$

There, $S(x-y)$ is the fully dressed quark propagating from point y to x, $D^{AB}_{\mu\nu}(x-a) = \frac{\delta A^B_\mu(a)}{\delta j^A_\mu(x)}$ is the dressed gluon propagator and $\frac{\delta^3\Gamma[A^A_\mu,\bar{q},q]}{\delta\bar{q}(c)\,\delta q(b)\delta A^B_\mu(a)}$ is the dressed 1-particle irreducible (*truncated*) quark - gluon vertex . Re-inserting all of these expressions in Eq. (2.3) and changing to momentum space by applying a Fourier transformation the following relation for the inverse quark propagator can be extracted:

$$\begin{aligned} S^{-1}(p,\mu) &= Z_2(\mu,\Lambda^2)\,S_0^{-1}(p,\Lambda^2) \\ &\quad - i\,g^2(\mu)\,Z_{1F}(\mu,\Lambda^2)\int_\varepsilon^\Lambda \frac{d^4k}{(2\pi)^4}\gamma_\mu\,\frac{\lambda^A}{2}\,S(k,\mu)\,i\,\Gamma^B_\nu(p,k,\mu)\,D^{AB}_{\mu\nu}(q,\mu), \end{aligned} \tag{2.6}$$

where the bare quark propagator $S_0^{-1}(p,\Lambda^2) = \left[i\not{p} + Z_m(\Lambda^2)m\right]$ was introduced. The gluon momentum q is given as the difference between the internal and external quark momenta: $q = k - p$. This is the Dyson-Schwinger equation for the quark propagator which is pictorially shown in Fig. (2.1). It is also known as the QCD gap equation[1, 19, 40]. The solution to this equation, the quark propagator, can now be written in terms of its intrinsic structures. While propagating through space-time the quark does not change color or flavor because only self interactions occur and the strong interaction is flavor-blind. Therefore it is possible to implicitly specify the color and flavor structure in the quark and write the general solution of the related DSE as

$$S_{\alpha\beta ABab}(p) = S_{\alpha\beta}(p)\otimes\frac{1}{\sqrt{N_c}}\delta_{AB}\otimes\frac{1}{\sqrt{N_f}}\delta_{ab}, \tag{2.7}$$

where only the Lorentz/Dirac structure has not been resolved in detail. It is now possible to solve this equation by making a suitable *ansatz* for $S_{\alpha\beta}(p,\mu)$ which is based on the involved covariant structures. Eq. (2.8) shows a way of applying such an *ansatz* and further extract two dressing functions which depend solely on the quark momentum p squared (and the renormalization scale μ). We omit the Lorentz indices in the following for brevity, writing them explicitly if necessary or advantageous for the reader. A second form, which

Figure 2.1: The Dyson-Schwinger equation for the quark propagator in pictorial form; straight and wiggly lines denote quark and gluon propagators respectively. Filled circles denote the fully dressed gluon propagators and the fully dressed quark-gluon vertex, empty circles the fully dressed quark propagator. The external momentum p in the first two graphs has been omitted for brevity.

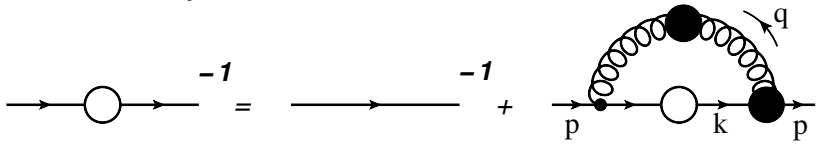

incorporates, of course, the same Dirac structure, is obtained by introducing a, to A inverse, dressing function $Z(p^2)$ and the mass function $M(p^2)$

$$S(p,\mu) = \underbrace{\left[\frac{1}{i\not{p}A(p^2,\mu^2) + B(p^2,\mu^2)\mathbb{1}_D}\right] = \frac{-i\not{p}A(p^2,\mu^2) + B(p^2,\mu^2)\mathbb{1}_D}{p^2A(p^2,\mu^2)^2 + B(p^2,\mu^2)^2}}_{\text{form 1}} = \tag{2.8}$$

$$= \overbrace{-i\not{p}\frac{Z_f(p^2,\mu^2)}{p^2 + M(p^2)^2} + \frac{Z_f(p^2,\mu^2)\,M(p^2)}{p^2 + M(p^2)^2}\mathbb{1}_D}^{\text{form 2}}. \tag{2.9}$$

As both of them are equally valid because they are all expressions for $S(p,\mu)$ it is of course possible to switch between the two forms by simple applying the relations between the dressing functions, e.g. $Z_f(p^2,\mu^2) = 1/A(p^2,\mu^2)$. We will stick to the first, solving for $A(p^2,\mu^2)$ and $B(p^2,\mu^2)$ but give plots for the dressing functions $Z_f(p^2,\mu^2)$ and $M(p^2)$. So inserting *form* 1 into equation (2.6) leads to

$$\begin{aligned}\left[i\not{p}A(p^2) + B(p^2)\mathbb{1}_D\right] &= Z_2(\mu,\Lambda^2)\,\left[i\not{p} + m_0(\Lambda^2)\right] \\ &- i\,g^2(\mu)\,Z_{1F}(\mu,\Lambda^2)\,\frac{N_C^2-1}{2N_C}\int_\varepsilon^\Lambda \frac{d^4k}{(2\pi)^4}\gamma_\mu\left[\frac{1}{i\not{k}A(k^2) + B(k^2)}\right]\,i\,\Gamma_\nu(p,k,\mu)\,D_{\mu\nu}(q,\mu),\end{aligned} \tag{2.10}$$

where we have re-inserted the expression for the bare quark propagator ($S_0^{-1}(p,\Lambda^2)$) and left aside the μ-dependence of the dressing functions for brevity. Further the color structures of the dressed quark-gluon vertex and the gluon propagator were extracted and traced-over using

$$i\,\Gamma_\nu^B(p,k,\mu) = \frac{\lambda^B}{2}\,i\,\Gamma_\nu(p,k,\mu) \qquad\qquad D_{\mu\nu}^{AB}(q,\mu) = \delta^{AB}\,D_{\mu\nu}(q,\mu), \tag{2.11}$$

obtaining

$$\mathrm{tr}_C\left[\frac{\lambda^A}{2}\frac{\lambda^A}{2}\right] = \frac{N_C^2-1}{2N_C} = C_F, \tag{2.12}$$

with C_F the Casimir invariant of the color group $SU(N_C)$. To solve Eq. (2.10) it is necessary to know already the dressed gluon propagator and the full quark-gluon vertex by having solved their Dyson-Schwinger equations before. This however turns out to be a even more laborious task than solving the quark. Therefore one needs to find a way to simplify the problem to a treatable form introducing *ansaetze* for both the gluon propagator $D_{\mu\nu}(q,\mu)$ and the quark-gluon vertex $\Gamma_\nu(p,k,\mu)$.

2.2 The Rainbow Truncation and Modeling $\mathcal{G}((k-p)^2)$

As pointed out already at the end of the previous section both the dressed gluon propagator and the dressed quark-gluon vertex are needed to solve the quark Dyson-Schwinger equation. The latter can be expressed into twelve Lorentz covariants and their related Lorentz invariants $T_i(p,k)$:

$$i\Gamma_\nu(p,k) = \gamma_\nu\, T_1(p,k) + (p+k)_\nu\, T_2(p,k) + (\not{p}+\not{k})(p+k)_\nu\, T_3(p,k) + \ldots, \tag{2.13}$$

where we neglected the dependence on the scale μ for brevity.
In general the fully dressed vertex is determined by its Dyson-Schwinger equation. Nevertheless to solve this DSE in full glory is a difficult task and has not been resolved yet. To obviate calculating the vertex including the entire Lorentz structure it is possible to employ an *ansatz*. Therefore let's recall the case of the quark-photon vertex in QED which in order to ensure gauge invariance has to fulfill a Ward-Takahashi identity (WTI) [41, 42]

$$(p-k)_\nu\, \Gamma_\nu(p,k) = S^{-1}(p) - S^{-1}(k). \tag{2.14}$$

Inserting now the expression of the fully dressed quark propagator the simplest solution for Γ_ν fulfilling the WTI is given by a longitudinal term, the Ball-Chiu vertex [43]

$$\begin{aligned} i\,\Gamma^{BC}_\nu(p,k) = {} & \frac{A(p^2,\mu)+A(k^2,\mu)}{2}\gamma_\nu - i\frac{B(p^2,\mu)-B(k^2,\mu)}{p^2-k^2}(p+k)_\nu \\ & + \frac{1}{2}\frac{A(p^2,\mu)-A(k^2,\mu)}{p^2-k^2}(\not{p}-\not{k})(p+k)_\nu. \end{aligned} \tag{2.15}$$

However, in general the full quark-gluon vertex can also be written as the bare vertex γ_ν plus a self-energy correction Λ_ν (c. f. Eq. (2.16))

$$\Gamma_\nu(p,k) = Z_{1F}\,\gamma_\nu + \Lambda_\nu. \tag{2.16}$$

The relevant step in the Rainbow truncation is to replace the complex structure, shown e.g. in Eq. (2.13), or equally the difficult self-energy part of Eq. (2.16), by the projection

onto a simple structure like the bare vertex γ_ν dressed by a non-perturbative function that solely depends on the exchanged gluon momentum q^2 [44]

$$\Gamma_\nu(p,k) = \gamma_\nu \left(Z_{1F} + \Lambda(q^2) \right). \tag{2.17}$$

Equivalently also a form like the following has been used in the literature [45]

$$\Gamma_\nu(p,k,\mu) = \Gamma_\nu^{\mathrm{Abel}}(p,k,\mu) \underbrace{G^2(q^2,\mu)\widetilde{Z}_3(\mu,\Lambda^2)}_{\Gamma^{\neg\mathrm{Abel}}(q^2,\mu)}, \tag{2.18}$$

where the Abelian part can be given by the construction in Eq. (2.15) or, as used later on, the bare vertex. The non-Abelian part shows an *ansatz* introducing ghost dressing G and renormalization $\widetilde{Z}_3$ functions as multiplicative factors to the Abelian structure. All of the information concerning the quark-gluon vertex presented on the last pages is considered in Landau gauge except Eqn. (2.13) and (2.16), which are valid gauge-independently. Also in Landau gauge the gluon propagator is given by an expression including the gluon dressing function $D(q^2)$ and a transversal projector:

$$D_{\mu\nu}(q,\mu) = -\frac{D(q^2,\mu)}{q^2}\left(\delta_{\mu\nu} - \frac{q_\mu q_\nu}{q^2}\right) = D(q^2,\mu)\, D_{\mu\nu}^{\mathrm{free}}(q^2). \tag{2.19}$$

Collecting now the expressions for the full quark-gluon vertex in Eq. (2.18) and the dressed gluon propagator in Eq. (2.19) the entire information from the Yang-Mills sector can be absorbed into a new quantity defined as follows:

$$\frac{\mathcal{G}(q^2,\mu)}{4\pi} = \alpha(q^2) := \frac{g^2(\mu)}{4\pi} \underbrace{Z_{1F}\widetilde{Z}_3}_{=Z_2} D(q^2,\mu) G^2(q^2,\mu). \tag{2.20}$$

This is the renormalization-point dependent running coupling in Landau gauge QCD.
Re-inserting Eqs. (2.18),(2.19) and Eq. (2.20) into the quark Dyson-Schwinger equation (one of Eqs. (2.6) - (2.10)) e.g. Eq. (2.6) yields

$$\begin{aligned} S^{-1}(p,\mu) &= Z_2(\mu,\Lambda^2)\, S_0^{-1}(p,\Lambda^2) \\ &\quad - \frac{1}{3\pi^3}\int_\varepsilon^\Lambda d^4k\, 4\pi\, \alpha(q^2)\, D_{\mu\nu}^{\mathrm{free}}(q,\mu)\gamma_\mu\, S(k,\mu)\, i\,\Gamma_\nu^{\mathrm{Abel}}(p,k,\mu). \end{aligned} \tag{2.21}$$

Choosing as a first approximation the bare quark propagator in the WTI (Eq. (2.14)) the bare vertex can be employed as the sole term contributing to the structure of the quark-gluon vertex in the, up to now not known, related piece in the quark DSE: $i\,\Gamma_\nu^{\mathrm{Abel}} = \gamma_\nu$. It can be shown (e.g. [40]) that this fulfills the statement of a renormalization-point independent mass function for the quark $M(p^2)$ in Landau gauge if an additional factor of Z_2 appears next to the bare vertex γ_ν.

Figure 2.2: Diagrammatic representation of the quark DSE in Rainbow truncation

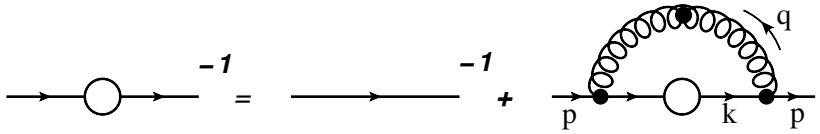

With the quark-gluon vertex and the gluon propagator specified all unknown variables have been at least partially illuminated and the left over unknown pieces are put into one function $\mathcal{G}(q^2)$

$$\begin{aligned} Z_{1F} \int_\varepsilon^\Lambda \frac{d^4k}{(2\pi)^4}\, g^2\, D^{AB}_{\mu\nu}(q) \frac{\lambda^A}{2} \gamma_\mu S(k) \Gamma^B_\nu(p,k) \\ \longrightarrow \quad Z_2(\mu,\Lambda^2) \frac{4}{3} \int_\varepsilon^\Lambda \frac{d^4k}{(2\pi)^4}\, \mathcal{G}(q^2)\, D^{\text{free}}_{\mu\nu}(q)\, \gamma_\mu S(k) \gamma_\nu, \end{aligned} \tag{2.22}$$

including

$$D^{\text{free}}_{\mu\nu}(q) = \frac{T_{\mu\nu}}{q^2} = \frac{1}{q^2}\left(\delta_{\mu\nu} - \frac{q_\mu q_\nu}{q^2}\right),$$

with $\mathcal{G}(q^2)$ being the only unknown function. Going back to Eq. (2.10) using the obtained information on the quark-gluon vertex and the gluon propagator needed to solve that equation and using again *form* 1 of equation (2.8) we can separate the quark DSE into two integral equations for the dressing functions $A(p^2)$ and $B(p^2)$. Thereby the only two pieces left to solve are the involved Dirac structure and the function $\mathcal{G}(q^2)$

$$\begin{aligned} S^{-1}(p,\mu) = Z_2(\mu,\Lambda^2)\, S_0^{-1}(p,\Lambda^2) \\ - \frac{Z_2(\mu,\Lambda^2)}{3\pi^3} \int_\varepsilon^\Lambda d^4k\, \mathcal{G}(q^2)\, D^{\text{free}}_{\mu\nu}(q,\mu) \gamma_\mu\, S(k,\mu)\, i\, \gamma_\nu, \end{aligned} \tag{2.23}$$

$$\begin{aligned} A(p^2) = Z_2 - Z_2 \frac{1}{4p^2} \frac{4}{3} \int_\varepsilon^\Lambda \frac{d^4k}{(2\pi)^4} \frac{A(k^2)}{k^2 A^2(k^2) + B^2(k^2)} \frac{\mathcal{G}((k-p)^2)}{(k-p)^2}, \\ \left(\delta_{\mu\nu}(k-p)^2 - (k-p)_\mu (k-p)_\nu\right)\ \text{tr}_D\left[\not{p}\gamma_\mu \not{k} \gamma_\nu\right] \end{aligned} \tag{2.24}$$

$$\begin{aligned} B(p^2) = Z_2\, Z_M\, m_0 + Z_2 \frac{1}{4} \frac{4}{3} \int_\varepsilon^\Lambda \frac{d^4k}{(2\pi)^4} \frac{B(k^2)}{k^2 A^2(k^2) + B^2(k^2)} \frac{\mathcal{G}((k-p)^2)}{(k-p)^2} \\ \left(\delta_{\mu\nu}(k-p)^2 - (k-p)_\mu (k-p)_\nu\right)\ \text{tr}_D\left[\gamma_\mu \mathbb{1} \gamma_\nu\right]. \end{aligned} \tag{2.25}$$

Finally we obtain the following two coupled integral equations to treat numerically:

$$A(p^2) = Z_2 + \frac{Z_2}{\pi^3}\int_\varepsilon^\Lambda dk\frac{k^2}{2}\int_{-1}^{1} d\cos(\theta)\,\frac{A(k^2)}{k^2A^2(k^2)+B^2(k^2)}\frac{\mathcal{G}((k-p)^2)}{(k-p)^2} \left[-\frac{2}{3}k^2 + \left(1+\frac{k^2}{p^2}\right)\sqrt{k^2}\sqrt{p^2}\cos(\theta) - \frac{4}{3}k^2\cos^2(\theta)\right] \tag{2.26}$$

$$B(p^2) = Z_2\,Z_M\,m_0 + \frac{Z_2}{\pi^3}\int_\varepsilon^\Lambda dk\frac{k^2}{2}\int_{-1}^{1} d\cos(\theta)\,\frac{B(k^2)}{k^2A^2(k^2)+B^2(k^2)}\frac{\mathcal{G}((k-p)^2)}{(k-p)^2} \left[k^2+p^2-2\sqrt{k^2}\sqrt{p^2}\cos(\theta)\right]. \tag{2.27}$$

Up to now the exact form of $\mathcal{G}((k-p)^2)$ has not been specified, so we present a simple model and a parametrization/model which are commonly used in Dyson-Schwinger - Bethe-Salpeter studies (e.g. [19, 46, 47]) as an ansatz. Both models yield the feature of dynamical chiral symmetry breaking in the infrared if tuned by suitable parameters D and ω (see Eq. (2.28) and (2.29)). The first one mentioned being just a Gaussian to model the gluon dressing [48] whereas the parametrization was used throughout different contributions to meson Bethe-Salpeter studies [19, 46, 47]. Within this work we will use in general the simple model as input for $\mathcal{G}((k-p)^2)$ leaving the second model to prospective investigations in the near future. Nevertheless we will give also results for the quark in this section that were obtained by using the parametrization introduced by Maris and Tandy in 1999 [47]

$$\frac{\mathcal{G}_{AWW}((k-p)^2)}{(k-p)^2} = \frac{4\pi\,D}{\omega^6}\,(k-p)^2\exp\left(\frac{-(k-p)^2}{\omega^2}\right), \tag{2.28}$$

$$\frac{\mathcal{G}_{MT}((k-p)^2)}{(k-p)^2} = \frac{4\pi\,D}{\omega^6}\,(k-p)^2\exp\left(\frac{-(k-p)^2}{\omega^2}\right) + \frac{4\pi\,\gamma_m\,\mathcal{F}}{\frac{1}{2}\ln\left[\tau+\left(1+\frac{(k-p)^2}{\Lambda^2_{\mathrm{QCD}}}\right)^2\right]}. \tag{2.29}$$

The second equation was first introduced by [46] where there was also a δ - function term involved that carried the infrared strength along with the finite width term also presented in Eq. (2.29). The latter as well as the one with the delta function preserves the one-loop renormalization group behavior of the quark Dyson-Schwinger equation and also show a characteristic asymptotic behavior in the ultraviolet [47]. For the present case of solving the quark we will simply stick to the chosen parameters given in that work to show some results in agreement with both the simple model study (as shown in [48]) and the more often considered parametrization of Eq. (2.29).

2.3 Results

In this section we give the obtained results for the quark dressing functions using the two versions of $\mathcal{G}((k-p)^2)$ given at the end of the last section (see Eq. (2.28) & Eq. (2.29)). We used $D = 1$ and $\omega = 0.5$ for the ab initio unknown parameters of the effective interaction $\mathcal{G}((k-p)^2)$. In Fig. (2.3(a)) we show the mass function $M(p^2) = B(p^2)/A(p^2)$ as a function of the positive, real, spacelike quark momentum squared. We give solutions for three different current quark masses, namely $m_0(\mu) \to 0$, $m_0(\mu) = 5$ MeV and $m_0(\mu) = 115$ MeV. These values stem from calculations in the MOM renormalization scheme at a related scale equal to the cut-off Λ (for the Gaussian model) or $\mu = 19$ GeV (for the model of [47]). In comparison the related numbers in the PDG are given in the $\overline{\text{MS}}$ scheme at a renormalization scale of 2 GeV. It is clearly visible that even in the limit for $m_0(\mu) \to 0$ dynamical chiral symmetry breaking is occurring due to a substantial increase in the quark mass function in the infrared regime. It is a typical feature of non-perturbative QCD and shows the quark mass generation due to the gluon coupling which can be interpreted as the so-called "constituent quark mass". The quark dressing function $Z(p^2) = 1/A(p^2)$ is plotted in Fig. (2.3(b)). Again we give results for three different current quark masses. Further interpretation and detailed knowledge can be found in several studies of the last years (in particular in [22, 40, 45, 48, 49, 50]).
In Fig. (2.3(c)) we change the effective interaction and add, as shown above, a logarithmic tail in the UV region. The results are therefore altered with respect to that change in $\mathcal{G}((k-p)^2)$. The quark mass function still obtains an substantial increase in the IR regime (i.e. around and below 1 GeV) but now decreases logarithmically in the ultraviolet. This is in agreement with the construction of $\mathcal{G}((k-p)^2)$ which is due to the wanted asymptotic behavior of $\alpha(q^2) \overset{k^2\to\infty}{\longrightarrow} \frac{\pi\gamma_m}{\ln k^2 \,/\, \Lambda^2_{QCD}}$ as constrained by one-loop perturbative QCD.
In the next section when dealing with the Bethe-Salpeter equation the quark propagator will be needed in general for complex momenta. However the analytic continuation may be difficult. Also, due to numerical treatment, the dressing functions $A(p^2)$ and $B(p^2)$ are only known on a finite grid of real positive momenta. Nevertheless also in the complex plane the quark must reduce to the free fermion propagator in the limit of large momenta p. In Fig. (2.3) a sketch of the complex momentum plane is shown. Due to the composite momentum dependence of the quark inside the Bethe-Salpeter equation the region where it has to be known changes from the real axis to a parabolic region in the complex plane. In addition complex conjugated poles are appearing at negative values of $\mathfrak{Re}(p^2)$ which request careful numerical treatment.

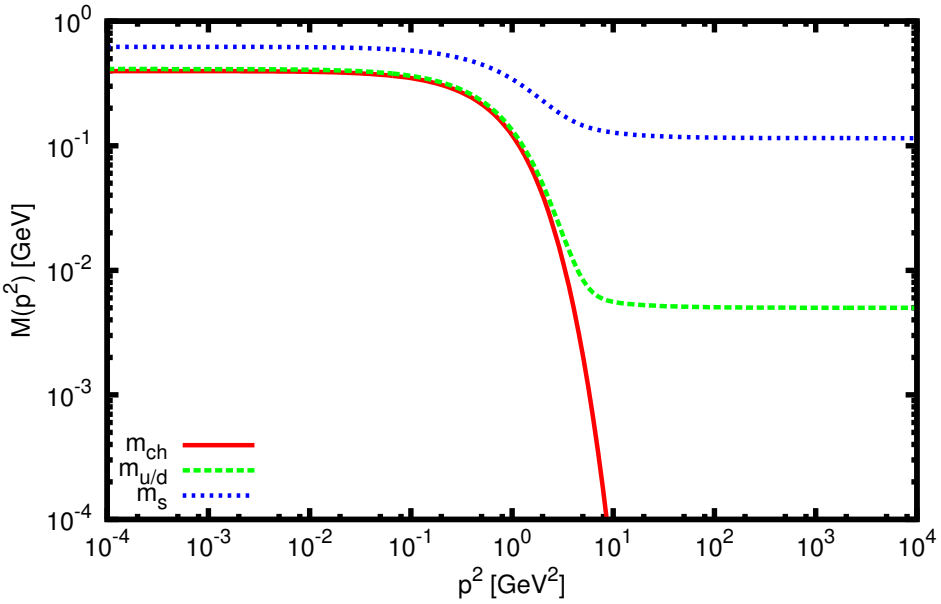

(a) The mass function $M(p^2)$ of the quark propagator using the simple Gaussian model for three different current quark masses m_0.

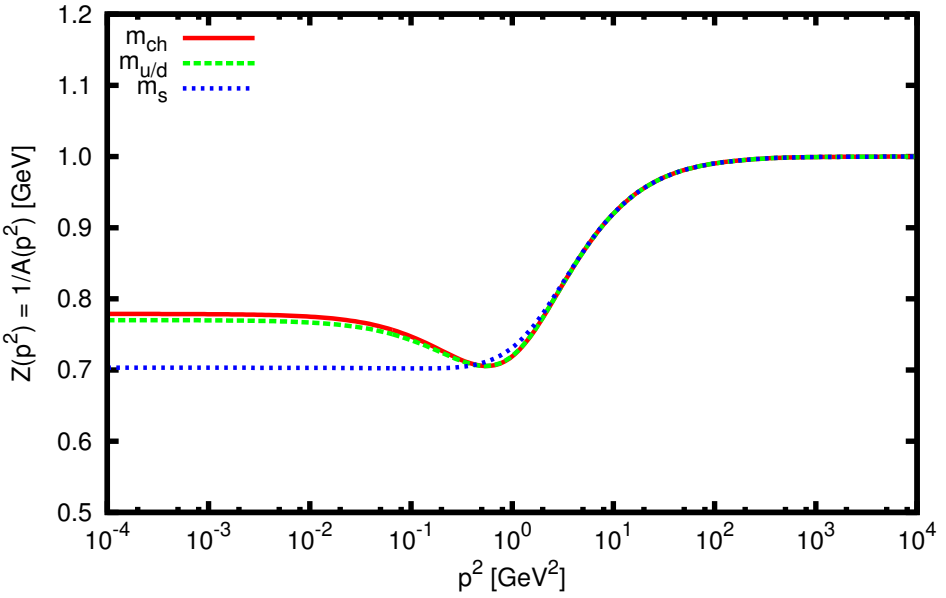

(b) The quark dressing function $Z(p^2)$ for $m_0 \to 0$ and $m_0 = 5$ and 115 MeV again using the Gaussian model and plotting for three different quark masses $m(\mu)$.

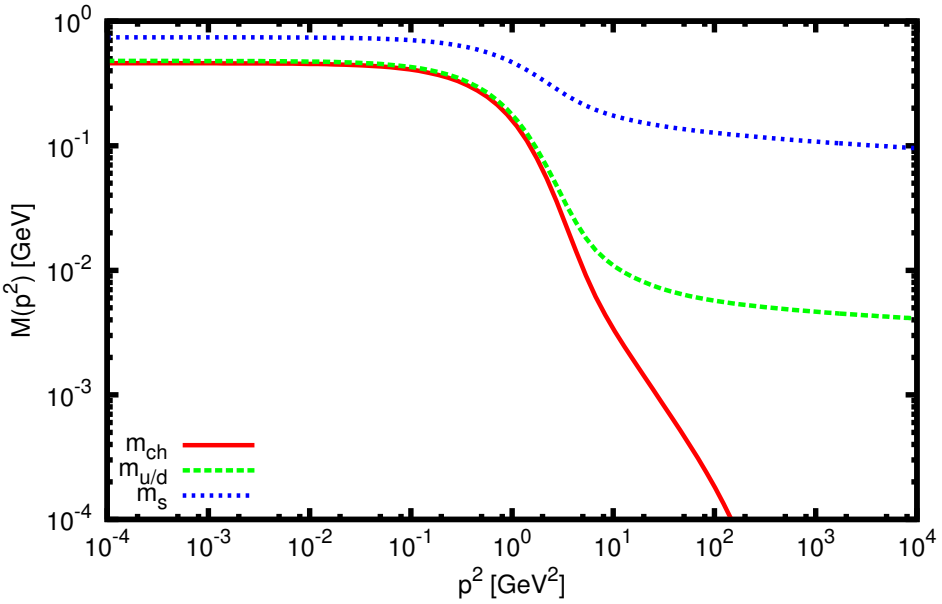

(c) The quark mass function $M(p^2)$ using the model of Maris and Tandy [47] for different values of the current quark mass $m(\mu)$.

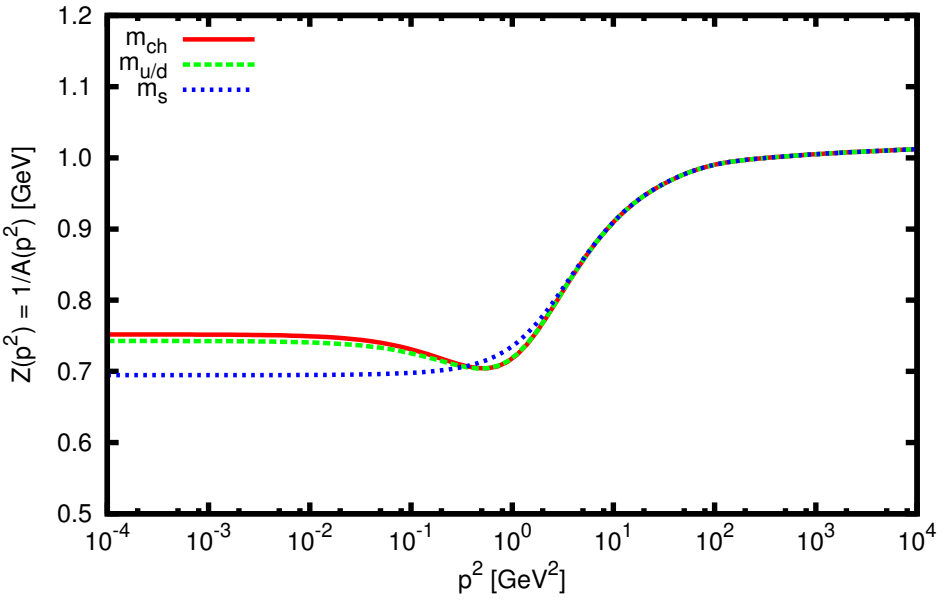

(d) The quark dressing function $Z(p^2)$ in the same approach. Again we give

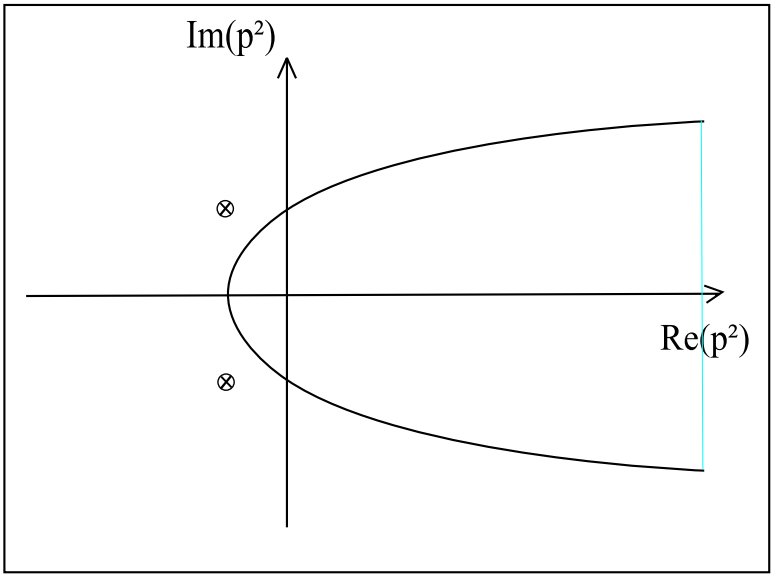

Figure 2.3: A sketch of the analytic behavior of the quark propagator in the complex p^2 plane as it is needed for the Bethe-Salpeter equation; the parabola indicates the region where it has to be calculated whereas the crossed circles indicate the appearing poles.

Chapter 3

Relativistic Bound States and the Bethe-Salpeter Equation

3.1 Derivation of the 4-point Dyson-Schwinger Equation and the homogeneous Bethe-Salpeter Equation

In this chapter we want to lay a hand on the derivation of bound states in the functional framework of Dyson-Schwinger and Bethe-Salpeter equations. For this to work we derive first the homogeneous Bethe-Salpeter equation (BSE) using further functional derivatives and the equations already stated in chapter 2. We thus arrive at an integral equation that has to be solved numerically. Finally we give explicit results for the scalar and pseudo-scalar case.

3.1.1 Obtaining the 4-point Green's Function

Having shown how to obtain the 2-point Green's function, in particular for the quark in QCD, we turn now to the 2-body problem. To obtain information on the level of Green's functions we need to consider not two but four derivatives. In the case of a fermion–anti-fermion system it is necessary to take three more derivatives of the master equation (1.26) with respect to the quark source at points y and y' and the anti-quark source at point x'. After several steps of algebra using various definitions and results from the previous sections the 4-point Green's function is obtained as follows: Being defined as the fourth derivative of the generating functional of connected Green's functions $W_{\text{conn}}[J_i]$, the 4-point connected Green's function is defined analogously to other Green's functions in chapter 2

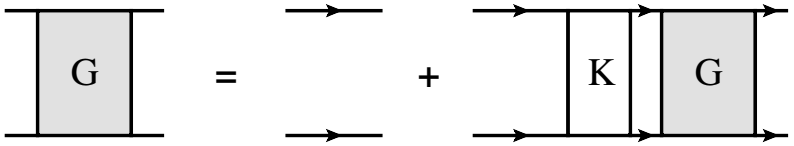

Figure 3.1: The 4-point fermion–fermion Green's function, also sometimes known as the inhomogeneous Bethe-Salpeter equation.

as

$$G^{(4)}(x,y;x'y') := \frac{\delta^{(4)}\, W[j^a_\mu,\eta,\bar\eta]}{\delta\eta(y')\,\delta\bar\eta(x')\,\delta\eta(y)\,\delta\bar\eta(x)}. \tag{3.1}$$

Bringing now the included pieces together and using an identity for the functional derivative of the product of $Z[A,q,\bar q]$ with $G^{(4)}(x,y;x'y')$ it is possible to arrive at the following Dyson-Schwinger equation for the 4-point Green's function $G^{(4)}(x,y;x'y')$

$$\begin{aligned}\left[Z_2\,(i\partial\!\!\!/_x - Z_m\,m) - e\,A\!\!\!/^a(x) - e\gamma_\mu \frac{\delta}{i\delta j^a_\mu(x)}\right] G^{(4)}(x,y;x'y')\Big|_{j^a_\mu=0} = \\ = \delta^4(x-y)S(x',y') - \delta^4(x-y')S(x',y).\end{aligned} \tag{3.2}$$

Including the result for the 2-point Green's function (c.f. 2.6)

$$(Z_2(\partial\!\!\!/_{x'} - Z_m m) - Z_{1F}\Sigma_{x'})\,S(x',y) = \delta^4(x'-y), \tag{3.3}$$

Eq. (3.2) becomes

$$\begin{aligned}(Z_2(\partial\!\!\!/_{x'} - Z_m m) - Z_{1F}\Sigma_{x'})\,(Z_2(\partial\!\!\!/_x - Z_m m) - Z_{1F}\Sigma_x)\,G^{(4)}(x,y;x'y') = \\ = \delta^4(x-y)\delta^4(x'-y') - \delta^4(x-y')\delta^4(x'-y) \\ + (Z_2(\partial\!\!\!/_{x'} - Z_m m) - Z_{1F}\Sigma_{x'})\left[e\gamma_\mu\frac{\delta}{\delta j^a_\mu(x)} - Z_{1F}\,\Sigma_x\right] G^{(4)}(x,y;x'y'),\end{aligned} \tag{3.4}$$

where Eq. (3.3) was inverted and the part in brackets multiplied to the left hand side of the equation. Further the term including the functional derivative was brought on the right-hand-side. Introducing now a convolution integral to define the kernel $K(x,x';z,z')$ (c.f. Eq. (3.5)) it is straightforward to obtain an equation, that will be called *inhomogeneous* Bethe-Salpeter equation

$$\begin{aligned}(Z_2(\partial\!\!\!/_{x'} - Z_m m) - Z_{1F}\Sigma_{x'})\left[e\gamma_\mu\frac{\delta}{\delta j^a_\mu(x)} - \Sigma_x\right] G^{(4)}(x,y;x'y')|_{j^a_\mu=} \\ =: \int d^4z\,d^4z'\,K(x,x';z,z')G^{(4)}(z,y;z',y').\end{aligned} \tag{3.5}$$

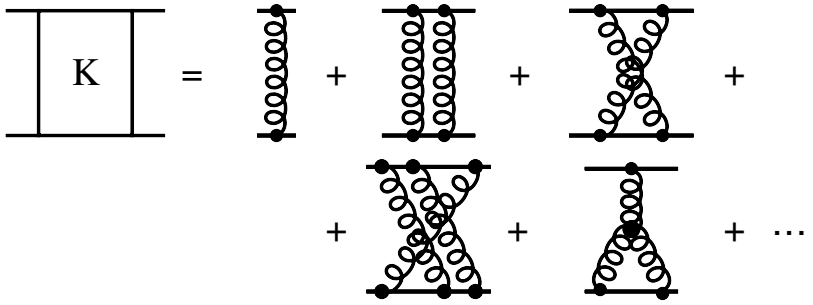

Figure 3.2: The first few terms of a skeleton expansion of the kernel K constructed out of 1-particle irreducible terms.

The kernel K is given through the sum of all 2-particle irreducible graphs which cannot be disconnected cutting two fermionic lines. The first few terms are visible in Fig. (3.2). Inserting the expression for K into Eq. (3.4) leads to the result for the 4-point function $G^{(4)}(x,y;x'y')$ as an inhomogeneous integral equation with kernel $K(x,x';z,z')$

$$\boxed{\begin{aligned}(Z_2(\not\partial_{x'} - Z_m m) - Z_{1F}\Sigma_{x'})\,(Z_2(\not\partial_x - Z_m m) - Z_{1F}\Sigma_x)\,G^{(4)}(x,y;x'y') = \\ = \delta^4(x-y)\delta^4(x'-y') - \delta^4(x-y')\delta^4(x'-y) \\ + \int d^4z\, d^4z'\, K(x,x';z,z')G^{(4)}(z,y;z',y').\end{aligned}} \tag{3.6}$$

Often it is also convenient to give the Bethe-Salpeter equation in momentum space. This can be done easily by Fourier transformation which is not explicitly given here but can be found in numerous studies about the subject [1, 22]. In addition we change to center-of-mass coordinates and introduce for the coordinate representation the center-of-mass coordinate X and the relative coordinate x given in the first line of Eq. (3.7) and their respective conjugated variables in momentum space, P and p listed below. With these definitions, namely

$$\begin{aligned} X &= \eta x + \bar\eta y \quad & x &= x - y \\ p_1 &= \eta P + p \quad & p_2 &= \bar\eta P - p \end{aligned} \qquad \eta + \bar\eta = 1, \tag{3.7}$$

whereas η and $\bar\eta$ are arbitrary momentum partitioning parameters, the 4-point Dyson-Schwinger equation and its solution, the 4-point Green's function can be re-expressed in terms of the introduced momentum space variables P and p

$$\boxed{\int \frac{d^4p'}{(2\pi)^4}\left[\tilde D(P,p,p') + \tilde K(P,p,p')\right]\tilde G^{(4)}(P,p',p'') = \delta^4(p-p'').} \tag{3.8}$$

Used is further a new variable $\tilde D(P,p,p')$ which is defined as the product of two inverse fermion propagators involved as the inhomogeneous term in the 4-point Dyson-Schwinger

equation. Its detailed definition can be seen below

$$\tilde{D}(P,p,p') := (2\pi)^4\,\delta^4(p-p')S^{-1}(p_1)\,S^{-1}(-p_2). \tag{3.9}$$

Thus we have arrived at a 4-point Dyson-Schwinger equation for a two-particle system and its solution, the 4-point Green's function in the coordinate and the momentum space. Nevertheless to solve the Dyson-Schwinger equation completely it is necessary to know the kernel-function K which is a priori a sum over infinitely many graphs and thus cannot be calculated easily if even possible. It is therefore necessary to truncate the kernel to a treatable form.
Moreover up to this point the equations used did not explicitly extract information on bound states. Nevertheless if there exists one it will of course contribute to the 4-point Green's function $G^{(4)}(x,y;x'y')$. These contributions and their extraction from the general Dyson-Schwinger equation for the 2-particle system will be the subject of the next section and is known as the homogeneous Bethe-Salpeter equation [51].

3.1.2 Extracting the Pole Structure – the homogeneous Bethe-Salpeter Equation

In the next few lines we will take a look on how bound states will appear in the 4-point Green's functions as intermediate states in scattering theory, give the resulting equation, called the *homogeneous Bethe-Salpeter equation* and apply a truncation to the kernel matrix K which is necessary to render the obtained system treatable. As a first step we return to a representation of the 4-point function as a vacuum expectation value $\langle T[\Phi(x_1)\dots\Phi(x_n)]\rangle$. To investigate intermediate bound states in e.g. a k to $n-k$ scattering we further consider only the case where $k<n$ fields Φ can all be time-ordered before the left over fields Φ_{k+1} to Φ_n. The time-ordered product can then be written as two time-ordered products with an Θ-function to account for the separation. In the case of an interacting fermion–anti-fermion system this can be written as

$$G^{(4)}(x,y;x'y') = \sum_\alpha \int \frac{d^3P}{(2\pi)^2\,2\omega}\,\langle 0|\,T\left[\psi_{(1)}(x)\psi_{(2)}(y)\right]|P,\alpha\rangle\,\langle P,\alpha|T\left[\bar{\psi}_{(1)}(x')\bar{\psi}_{(2)}(y')\right]|0\rangle \times \underbrace{\frac{-1}{2\pi i}\int_{-\infty}^{\infty} d\omega\,\frac{e^{-i\omega t}}{\omega+i\varepsilon}}_{\Theta(t)}. \tag{3.10}$$

We can now define a new function χ as a transition element from the vacuum containing two fields ψ and $\bar{\psi}$ into a bound state with total momentum P and internal quantum numbers α. χ will be called the *Bethe-Salpeter amplitudes*. Eqs. (3.11) - (3.12) show the definition

of the Bethe-Salpeter amplitudes and their re-expression in momentum variables. Further applying the transition to the center-of-mass frame and switching to momentum space variables, like in the previous section, we can re-express the 4-point Green's function

$$\begin{aligned}\chi(x,y,P) :&= \langle 0|T\left[\psi_{(1)}(x)\psi_{(2)}(y)\right]|P,\alpha\rangle \\ &= \chi(P,x)e^{-iP\cdot X},\end{aligned} \tag{3.11}$$

$$\chi(P,p) = \int \frac{d^4p}{(2\pi)^4}\,\chi(P,x)e^{i\,p\cdot x}, \tag{3.12}$$

$$\bar{\chi}(x',y',P) :\, = \langle P,\alpha|T\left[\bar{\psi}_{(1)}(x')\bar{\psi}_{(2)}(y')\right]|0\rangle. \tag{3.13}$$

Inserting these definitions and, as stated above, change to momentum space it is possible to obtain the following result for $G^{(4)}$:

$$\tilde{G}^{(4)}(P,p,p') = \sum_i \frac{i}{(2\pi)^4}\,\frac{\chi_P(P_i,p)\,\bar{\chi}_P(P_i,p')}{P^2+M_i^2+i\varepsilon}\bigg|_{P_i^2=-M_i^2} + \text{regular terms}(P,p,p'). \tag{3.14}$$

This expression can be re-inserted in Eq. (3.8) and after multiplying by $P^2+M_i^2$ and letting $P^2 \to -M_i^2$ (i.e. compare the residues at the pole $P^2=-M_i^2$) we obtain an integral equation for the *wavefunction* $\chi(P_i,p)$ which is called the *homogeneous Bethe-Salpeter equation for the amplitude*:

$$\int \frac{d^4p'}{(2\pi)^4}\left[\tilde{D}(P_i,p,p')+\tilde{K}(P_i,p,p')\right]\chi_P(P_i,p') = 0 \tag{3.15}$$

$$\chi_P(P_i,p) = S(p_1=p_+)\,S(-p_2=-p_-)\int \frac{d^4p'}{(2\pi)^4}\tilde{K}(P_i,p,p')\,\chi_P(P_i,p'). \tag{3.16}$$

More generally the entities $[\tilde{D}-\tilde{K}]$ and $G^{(4)}(P,p,p')$ in Eq. (3.8) can be expanded in powers of $(P^0-P_i^0)$ at the position of the pole. From this expansion it is possible to derive both the homogeneous BSE and the later discussed normalization condition if Eq. (3.8) is fulfilled with respect to the order $(P^0-P_i^0)^{-1}$ and to order $(P^0-P_i^0)^0$, respectively. Defining now the Bethe-Salpeter *vertex function* $\Gamma(P_i,p)$ as

$$\chi_P(P_i,p) =: S(p_1=\eta P_i+p)\,\Gamma_P(P_i,p)\,S(-p_2=\bar{\eta}P_i-p), \tag{3.17}$$

shifts the involved quark propagators $S(p_1)$ and $S(p_2)$ in Eq. (3.16) from outside the integral to the inside and so the homogeneous BSE becomes

$$[\Gamma(P,p)]_{ab} = \int \frac{d^4k}{(2\pi)^4}\tilde{K}^{cd}_{ab}(P;p,k)\;[S(k_+)\Gamma(P,k)S(-k_-)]_{dc}\,, \tag{3.18}$$

whereas a, b, c and d denote Lorentz indices. In addition the integration momentum has been changed to k for convenience. The quark propagators carry momentum $k_+ = k + \eta P$ and $k_- = k - \bar{\eta} P$ fulfilling $k_+ - k_- = P$ and $k = \bar{\eta} k_+ + \eta k_-$. The momentum partitioning fulfilling $\eta + \bar{\eta} = 1$ will be chosen to be $\eta = \bar{\eta} = \frac{1}{2}$ in the calculations. Pictorially the Bethe-Salpeter equation is shown in Fig. (3.3) also including the respective momenta. As in the section concerning the 4-point Dyson-Schwinger equation the kernel function K is not specified up to now. To solve the homogeneous BSE, present in whatever form, it is necessary to find a treatable form of this kernel, i.e. a *truncation*. Moreover as an input for the BSE one has to solve first the needed quark propagators in a parabolic region. The parabolic region is obtained as the quark dressing functions $A(p^2)$ and $B(p^2)$ are now needed as functions of complex momenta squared, i.e. $k_\pm^2 = k^2 - \frac{M^2}{4} \pm iMk_4$ (c.f. Fig. (2.3)).

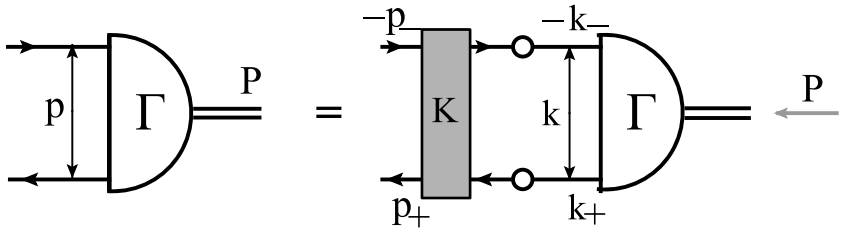

Figure 3.3: The homogenous Bethe-Salpeter equation in pictorial form also showing the included momenta.

In addition, QCD is also characterized by a rich intrinsic structure which is also reflected in the associated Green's functions of the theory as well as in the S-Matrix. Through the underlying symmetry groups of the involved structures, which can be identified as Lorentz, Dirac, flavor and color structures, objects in QCD carry a corresponding Lorentz, Dirac, flavor and color index. With this structures it is possible to expand first the QCD Green's functions in terms of the mentioned intrinsic entities and later also the Bethe-Salpeter amplitudes (BSA) as they inherit the same structure as well. This is linked to the fact that in QCD two types of irreducible representations, the *fundamental* (e.g. quarks, anti-quarks) and the *adjoint* (gluons), appear. These representations are connected with the Lie algebra of the related Lie group thus inheriting not only the same intrinsic but also the algebraic structure. This implies linear space properties and thus via the definition of a scalar product leads to orthogonality. In return it is possible to expand the group structure of the Green's functions onto a suitable basis. Although the Bethe-Salpeter amplitudes are not per definition defined as vacuum expectation values of fundamental fields they feature the Dirac, flavor and color structures of their parent 4-point Green's functions. In Eq. (3.19) and (3.20) this intrinsic structures of both the Green's function

and the Bethe-Salpeter amplitudes are sketched

$$\tilde{G}^{(4)}(p) = \sum_{\mu\alpha aA} F_{\mu\alpha aA}(p) \cdot [\mathbf{L}_\mu(p) \otimes \mathbf{D}_\alpha(p) \otimes \mathbb{s}^a(p) \otimes \mathbf{c}_A(p)]\,, \tag{3.19}$$

$$\Gamma_M(P,p) = \sum_i F^{P^2=-M^2;\,i}(p^2, p\cdot P)\, \tau_{M;i}(P,p,\gamma) \otimes \frac{1}{\sqrt{3}}\delta_{A\bar{B}} \otimes \mathbb{s}^I_{a\bar{b}}, \tag{3.20}$$

where first $\mathbf{L}$, $\mathbf{D}$, $\mathbb{s}$ and $\mathbf{c}$ correspond to elements of a particular representation of the underlying structure group, i.e. Lorentz, Dirac, flavor and color respectively. Further, in Eq. (3.20) for the BSA, τ_i^M represents the Dirac basis element(s) (also carrying Lorentz indices), while $\mathbb{s}^I_{ab}$ and δ_{AB} account for the specific flavor and color structure of the meson under consideration. How to obtain the different components of this decomposition is described in appendix A.2.

As we want to implement chiral symmetry and its dynamical breaking correctly, i.e. e.g. the pion as the Goldstone boson being massless in the chiral limit, it is necessary to truncate the quark propagator self-energy as well as the meson Bethe-Salpeter kernel consistently with this constraint. The axial-vector Ward-Takahashi identity (avWTI) [41, 42] ensures this correct implementation of chiral symmetry as well as its breaking (χSB) and relates the quark self-energy to the quark–anti-quark kernel in the pseudo-scalar BSE. In addition it is possible to obtain a generalized Gell-Mann–Oakes–Renner relation for all pseudo-scalar mesons and current quark masses [46, 52, 53] through the avWTI. The avWTI can be written as follows:

$$\{\gamma_5\,\Sigma(-p_-) + \Sigma(p_+)\,\gamma_5\}_{\alpha\beta} = -\int \frac{d^4k}{(2\pi)^4}\, K_{\alpha\gamma,\delta\beta}(P,p,k)\; \{\gamma_5\, S(-k_-) + S(k_+)\,\gamma_5\}_{\gamma\delta}\,. \tag{3.21}$$

A pictorial form is given in Fig. (3.4), where the crossed circles denote inserted γ_5's, white circles denote full propagator, grey ones full vertices and grey boxes represent the $q\bar{q}$-kernels. The approach of [54] represents a $q\bar{q}$-kernel derivation via functional derivatives of the quark

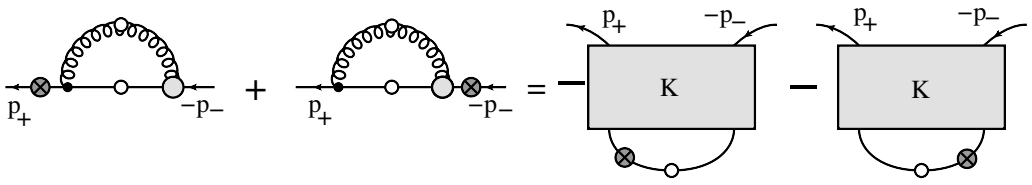

Figure 3.4: The axial-vector Ward-Takahashi identity: the white circles indicate full propagators, the grey ones full vertices and the crossed ones inserted γ_5-matrices.

self-energy. Following this approach also several other studies (e.g. [12, 47, 48, 53]) use the same construction of a vector-vector interaction $q\bar{q}$-kernel that fulfill the avWTI linking it to the quark propagator but model the remaining effective interaction in various ways. In

this work we will also simply consider this most trivial setup corresponding to the lowest order in the demanded symmetry preserving truncation scheme, i.e. a bare quark-gluon vertex $i\gamma_\mu$. It is directly linked to the truncation which was presented in Sec. 2.2, called the Rainbow truncation.
Taking this simple setup requiring the avWTI to be fulfilled one arrives at a gluon ladder exchange with bare quark-gluon vertices for the $q\bar{q}$-kernel. A detailed expression is given in the following equation:

$$K_{\alpha\gamma,\delta\beta}(P,p,k) = Z_2^2 \overbrace{\frac{4\pi\alpha(q^2)}{q^2}}^{\mathcal{G}(q^2)} \left(\frac{\lambda^a}{2}\right)_{AC} \left(\frac{\lambda^a}{2}\right)_{BD} (i\gamma_\mu)_{\alpha\gamma} \overbrace{\left(\delta^{\mu\nu} - \frac{q^\mu q^\nu}{q^2}\right)}^{=:T_q^{\mu\nu}} (i\gamma_\nu)_{\beta\delta}. \quad (3.22)$$

The function $\mathcal{G}$ (or equally α) thereby incorporates the gluon propagator and the quark-gluon dressing functions as well as the coupling strength g of QCD. The λ^a's account for the color structure and are of course the $SU(3)_C$ Gell-Mann matrices. Due to the isospin symmetry and equal masses of the contributing quarks the flavor structure does not contribute in this case. With this result the task to solve the Bethe-Salpeter equation is put forward in a treatable form. Only the function $\alpha(q^2)$ is still unknown. However it is identical to the function used in the calculation of the quark propagator in the Rainbow truncation through the connection of the avWTI. The truncation scheme is therefore named the *Rainbow-Ladder truncation* (RL).
In pictorial form the Bethe-Salpeter equation changes from Fig. (3.3) where the kernel function K was not known a priori to the form where a simple gluon-ladder exchange has been put in the place of the kernel function K (c.f. Fig. (3.5)).

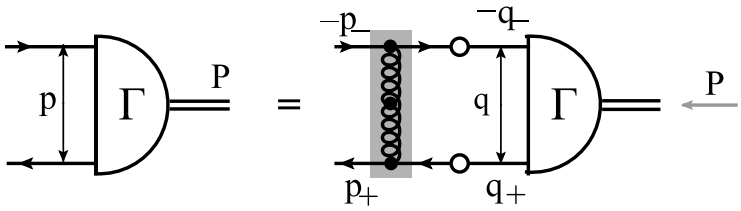

Figure 3.5: The homogeneous Bethe-Salpeter equation in pictorial form with a bare gluon exchange kernel shown emphasized in dark grey.

3.2 Normalization and the Pion Decay Constant

To obtain information on physical observables in the framework of Bethe-Salpeter equations it is further necessary to properly normalize the obtained amplitudes. Formerly the needed condition is obtained via the pole expansion of the 4-point Dyson-Schwinger equation being

fulfilled to order $(P^0 - P_i^0)^0$, i.e. that the residue in the 4-point $q\bar{q}$ Green's function is unity [40, 49]. The standard form has been first discussed by Leon and Cutkosky [55] and is built of two terms, one including the derivatives of the quark propagators with respect to Q^2 and the second taking the derivative of the kernel also with respect to the total momentum squared. There P^μ is the total momentum of the meson at the i^{th} pole, i.e. it fulfills $P^2 = -M_i^2$ (in Euclidean space-time). The bound state vertex functions $\Gamma_M^{i/j}$'s are calculated on the mass shell, i.e. resulting in a fixed value of P^2. Therefore the derivative in the first term only acts on the quark propagators $S(k)$. They carry different momentum $k_+ = k + \eta Q$ and $-k_- = k - \bar{\eta} Q$ respectively which shows the momentum partitioning of the total bound state (BS) momentum. Eq. (3.23) shows the described form of the normalization condition as it was first introduced by Leon and Cutkosky

$$\begin{aligned}\delta^{ij} = 2\,\frac{\partial}{\partial Q^2}\ \ \mathrm{tr}_D \int \frac{d^4\,k}{(2\pi)^4} \\ \Bigg[\, 3\Big(\bar{\Gamma}_M^i(-P,k) S(k+Q/2)\Gamma_M^j(P,k) S(k-Q/2)\Big) \\ + \int \frac{d^4\,q}{(2\pi)^4} [\bar{\chi}_M^i]_{ab}(-P,q) K_{cd;ba}(Q;q,k) [\chi_M^j]_{dc}(P,k)\Bigg]\,.\end{aligned} \tag{3.23}$$

In the Rainbow-Ladder truncation the kernel K is independent of the total momentum P and thus the second term in the normalization condition can be neglected which leaves only the first term to be calculated. In this case it can also be further simplified by substituting the BS amplitude for the product between the quark propagators and the vertex function (see therefore the definition of the vertex function, Eq. (3.17)). A second, but equivalent condition has been put forward by Nakanishi [56] which has received interest lately due to its applicability in beyond RL studies [57, 58],

$$\left(\frac{d\,\ln(\lambda)}{dP^2}\right)^{-1} = \mathrm{tr}_D \int_k 3\,\bar{\Gamma}(-P,k) S(k_+)\Gamma(P,k) S(k_-), \tag{3.24}$$

with λ being the associated eigenvalue which is introduced in the numerical treatment of the homogeneous Bethe-Salpeter equation. Further $\bar{\Gamma}(-P,k)$ is the charge conjugated Bethe-Salpeter vertex function defined via

$$\bar{\Gamma}(-P,p) := C\Gamma^T(-P,-p)C^{-1}, \tag{3.25}$$

with $C = -\gamma_2\gamma_4$, the charge conjugation matrix. The minus sign in the argument, in front of the total momentum P, is a convention to signal the opposite momentum flow in the vertex. Diagrammatically the normalization condition in the RL truncation is visible in Fig. (3.6). With the Bethe-Salpeter amplitudes now properly normalized it is possible to calculate physical observables like the leptonic decay constants. These constants are obtained in general [47] via

$$f_P\,P_\mu = \langle 0|\bar{q}^b\gamma_\mu\gamma_5 q^a|P^{ab}(P)\rangle. \tag{3.26}$$

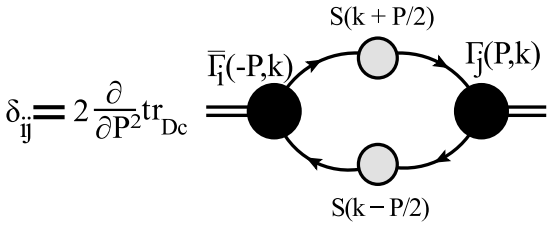

Figure 3.6: The normalization condition for the Bethe-Salpeter equation. Black filled circles and grey filled circles denote BS vertices and fully dressed quarks respectively.

In particular for the leptonic decay constant marking the pion coupling to the point axial field, i.e. the pion decay constant f_π, is given as

$$f_\pi = Z_2 \frac{3}{M_\pi^2}\ \mathrm{tr} \int \frac{d^4\,k}{(2\pi)^4} \Gamma_\pi(-P,k) S(k_+)\,\gamma_5 \not{P}\, S(k_-), \tag{3.27}$$

where the trace runs over Dirac matrices.Furthermore, in the chiral limit, it is possible to relate the quark mass dressing function B_χ to the first dressing function of the pion Bethe-Salpeter amplitude $\mathbb{E}_\pi$ via the pion decay constant [53] (see the appendix (A.2) for further information on the coefficient $\mathbb{E}$):

$$\mathbb{E}_\pi(P,p) = B_\chi(p^2)/f_\pi. \tag{3.28}$$

3.3 Numerical Treatment and Results

To obtain a solution for the Bethe-Salpeter equation for mesons it is necessary to handle the obtained equation numerically because an analytic exact solution is only possible in simple adaptions, e.g. the case of two scalar particles interacting via a scalar massless particle [23, 59]. In order to render the equation treatable with numerical methods one introduces a covariant Dirac basis $\tau_j(P,k)$ and expands the Bethe-Salpeter amplitudes in this basis as seen in Eq. (3.29). Thereby $\mathscr{F}_M^i(P^2,p^2,p\cdot P)$ is an element out of $\left\{\mathbb{E}_\mathrm{M}(P^2,p^2,p\cdot P), \mathbb{F}_\mathrm{M}(P^2,p^2,p\cdot P), \mathbb{G}_\mathrm{M}(P^2,p^2,p\cdot P), \mathbb{H}_\mathrm{M}(P^2,p^2,p\cdot P)\right\}$. Projecting on single basis elements τ_i leads to a matrix-vector multiplication structure in the space of the Dirac covariants. In addition it is also possible to add information about the flavor and color space properties of the amplitudes. Including all information concerning Dirac, Lorentz, flavor and color structures the Bethe-Salpeter amplitudes look like

$$\Gamma_M(P,p) = \sum_{i=1}^{N} \left\{\tau_{i;M}(P,p,\gamma)\right\}_{\alpha\beta} \mathscr{F}_M^i(P^2,p^2,p\cdot P) \ \otimes\ \frac{\delta_{A\bar{B}}}{\sqrt{3}} \ \otimes\ \mathbb{s}^I_{a\bar{b}}. \tag{3.29}$$

Eq. (3.29) is inserted into the Bethe-Salpeter equation (Eq. (3.18)) for the vertex function and all contributing terms on the right hand side (r.h.s.) of Eq. (3.18) except the invariant functions $\mathscr{F}_M^i(P^2, p^2, p \cdot P)$ are combined into one entity, which is called kernel matrix $\mathcal{K}$. This kernel matrix has the following form:

$$\mathcal{K}_j^i(P,p,k)\,\mathscr{F}_M^j(P^2,k^2,k\cdot P) := \\ \frac{4}{3}\int \bar{d}^4k \;\; \mathrm{tr}_D\Big[\tau_i(P,p)\,K(P,p,k)\,S^a(k+P/2)\tau_j(P,k)\,S^b(k-P/2)\Big]\,\mathscr{F}_M^i(P^2,k^2,k\cdot P), \tag{3.30}$$

with $\bar{d}^4k = \frac{d^4k}{(2\pi)^4}$. In addition the quark propagator function has to be known exactly for needed momenta in the complex plane where $\bar{\eta} = \eta = \frac{1}{2}$ has been chosen for the quark needed in a symmetric region in the complex plane. The quark propagator's, i.e. $S(k_\pm)$, dressing functions $A(k_\pm^2)$ and $B(k_\pm^2)$ thus have to be known in a parabolic region in the complex plane because of P in $k_\pm$ is equal to $P = iM$. The vertex of this parabola can be identified to be $x_0 = (-\frac{1}{4}M^2, 0)$ in Euclidean space-time having used $\eta^2 = \bar{\eta}^2 = \frac{1}{4}$.

Putting now Eq. (3.30) back into the Bethe-Salpeter equation using several discussed expansions one obtains a matrix-vector multiplication in the covariant basis $\tau_i(P,p)$. Each element of the matrix therefore includes certain Dirac basis elements, flavor and color structure and the four dimensional integral over k-space. The BSE takes the form

$$\mathscr{F}^{i,\mathcal{A}} = \mathcal{K}_{j,\mathcal{B}}^{i,\mathcal{A}}\,\mathscr{F}^{j,\mathcal{B}}. \tag{3.31}$$

$\mathcal{A}$ and $\mathcal{B}$ are multi-indices that represent the discretized momentum dependence needed numerically to treat the four dimensional integral involved. The i and j indices label the components. To solve this matrix-vector multiplication it is necessary to remember that the homogeneous Bethe-Salpeter equation is only valid on the mass shell and fulfills the condition $P^2 = -M_i^2$. The kernel matrix depends, as also the invariant functions $\mathscr{F}^i$ do, on P^2 and $k\cdot P$ as well as k^2 and $k\cdot p$. As it is therefore of need to know the value of P^2 for a certain bound state a priori to be able to evaluate the kernel matrix, it is necessary to pursue the following strategy: A suitable approach to obtain a valid bound state with mass M_i is to investigate the spectrum of $\mathcal{K}$ with respect to P^2, i.e. omit fixing P^2 ab initio but search for a certain P^2 where the BSE is fulfilled. Thus one obtains an eigenvalue problem for the matrix $\mathcal{K}$ depending on P^2. The homogeneous BSE is obtained if a certain value for P^2 gives an eigenvalue of $\lambda = 1$

$$\lambda(P^2)\vec{\mathcal{F}}(P^2,p^2,P\cdot p) = \mathcal{K}(P^2,p^2,k^2,P\cdot k,P\cdot p,p\cdot k)\cdot\vec{\mathcal{F}}(P^2,k^2,P\cdot k). \tag{3.32}$$

The corresponding eigenvectors are the Bethe-Salpeter vertex functions spanned in the Dirac basis $\tau_{i;M}(P,p)$.
Fig. (3.7) shows the masses of the iso-scalar σ meson and the pseudo-scalar pion both

calculated for different current quark masses m_0 between the chiral limit and the strange quark mass around 100 MeV. In Fig. (3.7) we name the state a "bare" state because we want to avoid confusion between the investigated iso-scalar $q\bar{q}$ state and the experimental σ. Moreover, the latter has been shown to miss the typical $\bar{q}q$-behavior in the large N_c-limit [31, 32] and therefore the "bare" state is not expected to match the experimentally observed properties e.g. the typical broad width expected for the σ. Nevertheless the result for the pion is in good agreement with the Gell-Mann–Oakes–Renner relation which demands the pion to be massless in the chiral limit. This is clearly visible in the down left corner. Further the iso-scalar $q\bar{q}$ state has a value around 660 MeV for a current quark mass of 5 MeV and is not massless in the chiral limit because it is not protected by chiral symmetry. Further detailed calculations in the discussed approach and related interpretations have been investigated already and can be found in numerous studies [19, 40, 46, 47, 48, 49, 53].

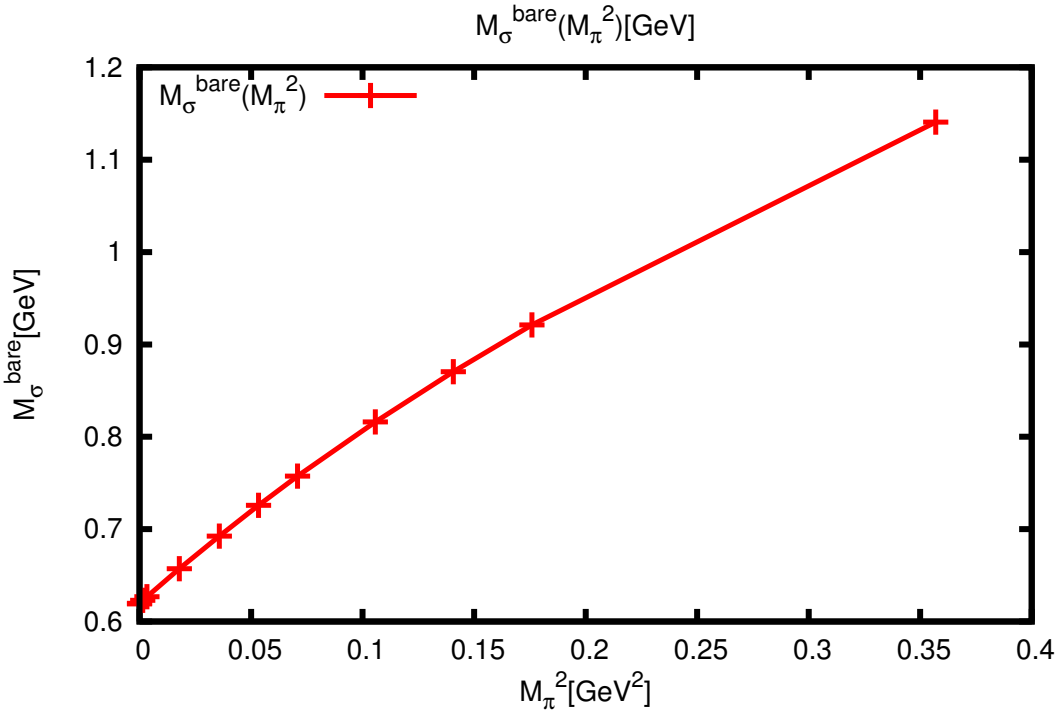

Figure 3.7: The masses of the bare sigma and the pion with rising current quark mass $m_0(\mu)$ using the Gaussian effective interaction of Chap.2 .

Chapter 4

Calculating Observables: the $\sigma \to \pi\pi$ Triangle Diagram

Having derived expressions for the quark propagator in chapter 2 and the homogeneous Bethe-Salpeter equation in chapter 3 it is possible to obtain information on hadronic decays through the calculation of related quantities. In particular we will give detailed information for the coupling strength of the σ into two pion and the width of the decaying σ into two pions. We will describe the mesonic decay via the triangle diagram, which has been used in perturbative studies [9, 10] as well as non-perturbative ones [12, 60, 19] to describe the specific hadronic 1- to 2-particle decay. In the first section of this chapter we will give an expression for the invariant amplitude of $\sigma \to \pi\pi$. Further we will solve for the color and flavor structure (details will be given in the appendix) of the invariant M-matrix (i.e. the invariant amplitude) and introduce new momentum variables P and Q whose definitions also can be found in the appendix. We will continue with giving explicit expressions for the coupling strength $g_{\sigma\to\pi\pi}$ and the decay width $\Gamma_{\sigma\to\pi\pi}$. Finally we will give some exemplary numbers for the decay under consideration (i.e. $\sigma \to \pi\pi$).

4.1 Building the Triangle Diagram

In the following, the quark propagator $S(p)$ and the normalized Bethe-Salpeter amplitudes $\Gamma(P, p)$ are used as input to calculate coupling strength and decay width of a specific process, i.e. the scalar σ meson decaying into two pions. Nevertheless we still deal with the "bare" σ particle which is a $\bar{q}q$-state and thus we do not expect finding values that actually fit with values in [2]. But first we derive some quantities needed to describe the process of a particle into two (or generally many) particles. We emphasize that we only

introduce terms like the S-matrix or the invariant amplitude $\mathcal{M}$ and that the reader is encouraged to read in standard literature like [1, 3, 4] if deeper knowledge is required.
We start with some general expressions on how to obtain the invariant amplitude (also called "M-matrix" in scattering theory [20]) starting from the S-matrix S. As is commonly known [3, 4, 20] in scattering theory the S-Matrix describes the unitary transition from asymptotic incoming states to outgoing states and is therefore also sometimes called the "infinite time evolution operator $U(\infty)$" [1, 3, 19]. Therefore it is possible to write a matrix element S_{fi} between an incoming state i and an outgoing state f as

$$S_{fi} = \langle f|i\rangle. \tag{4.1}$$

Further the matrix element can be decomposed into a part not interacting with anything else (i.e. a delta functional between incoming and outgoing state) and a part handling possible interactions, which is called the T-matrix. It is the latter part that is of interest because only there scattering occurs and particles in general interact with each other

$$S_{fi} = \delta_{fi} + T_{fi}. \tag{4.2}$$

Extracting the information on the energy-momentum conservation of the process under consideration the T-matrix splits into the part related to momentum and an invariant amplitude, also known as the "invariant transition matrix element" [20], still describing processes of (an) incoming particle(s) i scattering or colliding into final particle(s) f

$$T_{fi} = (2\pi)^4\, \delta^{(4)}(p_f - p_i)\, \mathcal{M}_{fi}. \tag{4.3}$$

As we deal in general with huge numbers of particles colliding in elementary particle experiments we need adequate quantities as observables. Such an observable is the scattering cross-section which describes the probability of finding a certain final state f after a scattering process of, in general, i incoming particles (given in Eq. (4.4)). Alongside a normalization factor the cross-section consists of an integral over phase-space and the absolute value squared of the invariant amplitude M_{fi}

$$d\sigma_f = \mathcal{N} \int d\Pi_f\, |\mathcal{M}_{fi}|^2. \tag{4.4}$$

Thus having expressed the cross-section in terms of the invariant amplitude we consider now the specific case of the matrix $\mathcal{M}_{fi}$ of a meson, described by its Bethe-Salpeter amplitude, into two mesons, also described by its respective Bethe-Salpeter vertex functions. We denote the three of them by $\Gamma_{1,2,3}$. Further sticking to the idea of the decay process being described by a diagram like the one represented in Fig. (4.1) we denote the invariant amplitude by a trace over color, flavor and Dirac structures over a four-dimensional Euclidean integral in momentum space. This is known as the *impulse approximation* introduced by Mandelstam [61]. The integrand is constructed by considering the Bethe-Salpeter vertex

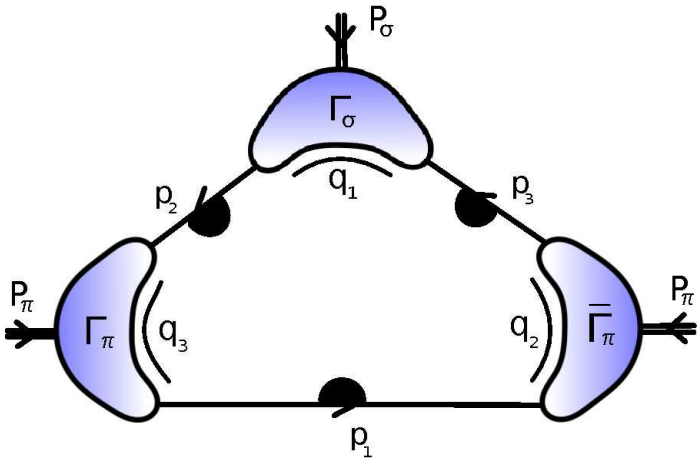

Figure 4.1: The Triangle diagram in a pictorial form describing the decay of the σ into two pions showing the internal quark loop and the included momenta.

functions of the initial and final states as well as the propagators connecting the amputated legs of the BS amplitudes. A general expression for such a process is given in (4.5)

$$\mathcal{M} = \mathrm{tr}_{Dfc}\left\{\int \bar{d}^4k\, \Gamma_2\, S_3\, \Gamma_1\, S_2\, \Gamma_3\, S_1\right\}. \tag{4.5}$$

If this concept is applied to the particular case of the the σ decaying into $\pi + \pi$ it is necessary to insert the related amplitudes for the iso-scalar σ and the pseudo-scalar pion. In the following we chose to replace Γ_1 with the incoming Bethe-Salpeter amplitude of the σ, Γ_σ, and $\Gamma_{2,3}$ with the associated pion amplitudes Γ_{π_i} and $\bar{\Gamma}_{\pi_i}$, one incoming, one outgoing. Further we also used the cyclic property of the trace to arrive at the following expression for the invariant amplitude $\mathcal{M}_{\sigma\to\pi\pi}$

$$\mathcal{M}_{\sigma\pi\pi} = \mathrm{tr}_{Dfc}\left\{\int \bar{d}^4k\, \Gamma_\sigma(P_\sigma, q_1)\, S_2(p_2)\, \Gamma_{\pi;3}(P_\pi, q_3)\, S_1(p_1)\, \bar{\Gamma}_{\pi;2}(-P_\pi, q_2)\, S_3(p_3)\right\}. \tag{4.6}$$

Isolating the color and flavor structure of Eq. (4.6) it is possible to evaluate the related traces in color and flavor space. A detailed description of how this is done can be found in the appendix (c.f. A.4). Here we will only concern ourselves with the resulting expressions and list them again for convenience.
The color trace is of a simple form since we deal only with hadronic states which need to be color-singlets. Thus the color trace is just a product of Kronecker - delta in color space resulting in a factor of N_c in general and in the case of QCD, as considered here, a factor of three

$$\mathrm{tr}_c\left\{\delta_\sigma^{A\bar{B}}\delta^{\bar{F}\bar{B}}\delta_\pi^{E\bar{F}}\delta^{\bar{D}E}\delta_\pi^{C\bar{D}}\delta^{AC}\right\} = \mathrm{tr}_c\left\{\mathbb{1}_c\right\} = N_c \overset{\text{here}}{=} 3. \tag{4.7}$$

Turning to the flavor structure the σ as an uncharged particle can decay into three different pairs of pions. The resulting flavor structure traces are given below and result all in a factor of $\frac{1}{\sqrt{2}}$ modulo a sign:

$\sigma \to \pi^0\pi^0$:

$$\mathrm{tr}_f\left\{\sigma\,\pi^0\,\pi^0\right\} = \mathrm{tr}_f\left\{\frac{1}{\sqrt{2}}\mathbb{1}_f\,\frac{1}{\sqrt{2}}\sigma_3\,\frac{1}{\sqrt{2}}\sigma_3\right\} = \frac{1}{2\sqrt{2}}\mathrm{tr}_f\left\{\mathbb{1}_f\right\} = \frac{1}{\sqrt{2}}, \tag{4.8}$$

$\sigma \to \pi^+\pi^-$:

$$\mathrm{tr}_f\left\{\sigma\,\pi^+\,\pi^-\right\} = \frac{1}{\sqrt{2}}, \tag{4.9}$$

$\sigma \to \pi^-\pi^+$:

$$\mathrm{tr}_f\left\{\sigma\,\pi^-\,\pi^+\right\} = -\frac{1}{\sqrt{2}}. \tag{4.10}$$

Having handled the up to now easy extractable color and flavor structure the resulting equation is written as the following (c.f. Eq. (4.11)). There new momentum variables were introduced which represent convenient variables to expand our investigation to another diagram in chapter five which involves the triangle of $\sigma \to \pi\pi$. The related investigation and transition from the former momentum dependence on the total and relative momenta of the BS amplitudes and the involved quark momenta to the new incoming total momentum P and the "relative" momentum between the outgoing pions can be found also in the appendix (c.f. A.3). Further we turn to a numerical treatment to extract information on the involved Dirac structure and the left over 4-dimensional integral and their respective solutions

$$\begin{aligned}
&\mathcal{M}_{\sigma\pi\pi}(P^2, Q^2, P\cdot Q) = \\
&\quad N_c\,\mathrm{tr}_{Df}\left\{\int \frac{d^4k}{(2\pi)^4}\,\Gamma_\sigma(P, k+Q/2)\,S_2(k-P/2+Q/2)\times\right. \\
&\qquad\qquad \times\,\Gamma_{\pi;3}(P/2-Q,\,k-P/4)\,S_1(k-Q/2)\times \\
&\qquad\qquad \left.\times\,\bar{\Gamma}_{\pi;2}(P/2+Q, k+P/4)\,S_3(k+P/2+Q/2)\right\}.
\end{aligned} \tag{4.11}$$

In the next section we turn to the description of two observables, the coupling strength and the Breit-Wigner decay width for the process under consideration and describe them by means of the invariant amplitude $\mathcal{M}_{\sigma\to\pi\pi}$ and eventually additional factors.

4.2 Coupling Strength & Decay Width

Having expressed the invariant amplitude in terms of BS amplitudes and quark propagators as obtained in the last section it is possible to use the relation between the cross-section

and the invariant amplitude to calculate the coupling strength $g_{\sigma\pi\pi}$ and the Breit-Wigner decay width $\Gamma_{\sigma\to\pi\pi}$ of the specific decay $\sigma \to \pi\pi$. First although the corresponding effective coupling strength between the σ and the two pions can be defined as the matrix element between the incoming $|\sigma(P_\sigma)\rangle$ and the outgoing $\langle\pi(P_\pi)\pi(P_\pi)|$ pion states (c.f. [62]) or equally the form factor F when all external particles are considered on-shell [19], i.e. $g_{\sigma\pi\pi} = F(P^2, Q^2, P\cdot Q)|_{P_i^2=-M_i^2}$ where $F(\ldots)$ is given in the invariant amplitude via $\mathcal{M}_{\sigma\pi\pi} = F(P^2, Q^2, P\cdot Q)\cdot\mathbb{1}$. So we can write the coupling strength as the already known traces over the 4-dimensional integral of the product of BS - amplitudes and quark propagators (c.f. Eq. (4.12)) fixing the bound state amplitudes of the σ and the π for their respective on-shell bound state mass values

$$\begin{aligned} g_{\sigma\pi\pi} &= \langle\pi(P_\pi)\pi(P_\pi)|\sigma(P_\sigma)\rangle = \\ &= \mathcal{M}_{\sigma\pi\pi}(P^2, Q^2, P\cdot Q)|_{P_i^2=-M_i^2} \\ &= N_c \frac{1}{\sqrt{2}} \operatorname{tr}_D \int_\varepsilon^\Lambda \bar{d}^4k \, \{\Gamma_\sigma(P, k+Q/2)\, S_2(k-P/2+Q/2)\times \\ &\qquad \times \Gamma_{\pi;3}(P/2-Q, k-P/4)\, S_1(k-Q/2)\times \\ &\qquad \times \bar{\Gamma}_{\pi;2}(P/2+Q, k+P/4)\, S_3(k+P/2+Q/2)\big\}\,. \end{aligned} \tag{4.12}$$

The color and flavor traces were again already solved in the last expression of Eq. (4.12) and again as in the case of the BSE we intend to solve the remaining Dirac structure and momentum space integrals by applying numerical techniques. As in Sec. 3.3 the BS amplitudes Γ_i are expanded in a covariant basis (c.f. appendix A.2) and their respective invariant amplitudes (c.f. Eq. (3.29)). The quarks are expressed in the already discussed dressing functions $A(p^2)$ and $B(p^2)$. With a little help from an algebraic solver [63] the Dirac structure can be solved and the remaining integration can be executed numerically. Results for the coupling strength will be given in the last section of this chapter. In addition again considering a the scalar σ-particle decaying into two pions it is possible to calculate a Breit-Wigner decay width for this particular process. It is advantageous to link the Breit-Wigner decay width to the scattering cross-section given as follows in Eq. (4.13)

$$\Gamma = \frac{1}{2M}\sum_f \int d\Pi_f \, |\mathcal{M}_{fi}|^2. \tag{4.13}$$

Thereby the integral runs over the phase-space of final states $\int d\Pi_f$. The variable M is the mass of the decay particle and $\mathcal{M}_{fi}$ is the already discussed invariant amplitude obtained as above (Sec. 4.1). We are left to obtain an expression for the phase-space integral. For a process like the decay of the σ into two final particles, the pions, the phase-space integral is given through a double integral over the as incoming defined outgoing momenta k_2 and k_3. Further in Eq. (4.14) an energy-momentum conservation delta functional is present and the former 4-dimensional integration has been split into space-like and time-like integrations

with the time-like ones already evaluated

$$\int d\Pi_f = \int \bar{d}^3\vec{k}_2 \int \bar{d}^3\vec{k}_3 \, \frac{(2\pi)^4 \, \delta^{(4)}(k_1 + k_2 + k_3)}{(-2i)\sqrt{M_2^2 + \vec{k}_2^2}(-2i)\sqrt{M_3^2 + \vec{k}_3^2}}. \tag{4.14}$$

The delta functional further simplifies the expression and leaves only one integration over $\vec{k}_2$ and a one-dimensional delta functional over the time-like components

$$\int d\Pi_f = -\int \bar{d}^3\vec{k}_2 \, \frac{2\pi}{4\sqrt{M_2^2 + \vec{k}_2^2}\sqrt{M_3^2 + \vec{k}_2^2}} \, \delta\left(M_1 - \sqrt{M_2^2 + \vec{k}_2^2} - \sqrt{M_3^2 + \vec{k}_2^2}\right). \tag{4.15}$$

It is then possible to separate the radial and angular parts of the remaining integral and solve the angular part in a straight forward manner. The left over integral in $d(\sqrt{\vec{k}_2^2})$ is again solved with the help of the apparent delta-functional

$$\int d\Pi_f = -\frac{1}{4}\int \frac{d^2\Omega}{(2\pi)^2} \int d\left(\sqrt{\vec{k}_2^2}\right) \, \frac{\vec{k}_2^2}{\sqrt{M_2^2 + \vec{k}_2^2} + \sqrt{M_3^2 + \vec{k}_2^2}} \, \delta(\sqrt{\vec{k}_2^2} - \xi). \tag{4.16}$$

Finally a general expression for the phase-space integral of a particle with mass M_1 decaying into two particles with masses M_2 and M_3 can be given and is shown in Eq. (4.17)

$$\int d\Pi_f = -\frac{\xi}{4\pi \, M_1}. \tag{4.17}$$

whereas ξ is given by the expression in Eq. (4.18) in terms of the three bound state masses $M_1,\ M_2,\ M_3$

$$\xi = \frac{\sqrt{(M_1 + M_2 + M_3)(M_1 - M_2 + M_3)(M_1 + M_2 - M_3)(M_1 - M_2 - M_3)}}{2M_1} \tag{4.18}$$

$$= \lambda(M_1^2, M_2^2, M_3^2), \tag{4.19}$$

$\lambda(\ldots)$ being the *Källen* function and the bound state masses squared of the incoming and outgoing particles, i.e. M_i^2, appearing as arguments. In the present case where the involved pions are considered in the iso-symmetric limit and thus all share the same mass one deals

with two identical final particles and M_2 can be set equal to M_3. Thus Eq. (4.17) turns into an expression of only the mass of the decaying particle and the mass of one of the final particles, e.g. M_2. In the case of the considered hadronic decay of the σ into two pions the equation changes accordingly whereas M_1 is substituted by the mass of the σ meson and M_2 is the mass of the pseudo-scalar bound state, i.e. the pion

$$\int d\Pi_f = -\frac{1}{8\pi}\sqrt{1 - \frac{4M_\pi^2}{M_\sigma^2}} \tag{4.20}$$

Recombining the obtained expression for the phase-space integral with the other needed components for Eq. (4.13) and calculating the sum over possible final states resulting in a factor of three it is possible to obtain a final expression for the Breit-Wigner decay width. The factor three is possible due to identical results with respect to color space and only a sign difference in the possible decays in flavor space

$$\boxed{\Gamma_{\sigma\to(\pi\pi)} = 3\, g_{\sigma\pi\pi}^2\, \frac{\sqrt{1 - 4M_\pi^2/M_\sigma^2}}{16\pi M_\sigma}.} \tag{4.21}$$

4.3 Results

In this section we will present some ideas on how to arrive at results for the discussed coupling strength $g_{\sigma\pi\pi}$ and the decay width $\Gamma_{\sigma\pi\pi}$. We will only investigate one set of parameters as needed for the effective coupling in the quark DSE and meson BSE and fix the mentioned parameters to $D = 1$ and $\omega = 0.5$. Further we will first model the pion Bethe-Salpeter amplitudes for the pion through the related quark-mass dressing functions of the quark propagators but in general calculate the triangle including the full structure of all amplitudes and propagators. Moreover, in principle it will be necessary to test for different settings, i.e. alter the choice of D and ω, choose other forms for the effective coupling, as well as also include contributions beyond the Rainbow-Ladder approximation to yield qualitative and quantitative results that are model and truncation independent.
Further, if we take a look at the involved momenta of the pion BS amplitudes, it is clearly visible that they can in general occupy complex values. Even though the pions can be calculated at the soft point, i.e. $P^2 = -M_i^2$, and in fact that is what we have done, the respective relative momentum stays complex. Therefore as we know the BS amplitudes only for real relative momenta k (or p), it is necessary to think of a analytic continuation of the BS amplitudes to complex relative momentum if the total momentum P_π stays fixed. A suitable method to accomplish this has been investigated and applied in [19] and we just apply the same techniques to alter the needed BS amplitudes for the pions accordingly.
From known experimental measurements of the $f_0(500)$ it is possible to infer that, for a mass of $M_\sigma \sim 420 - 550$ MeV and a decay width of $\Gamma_{\sigma\to\pi\pi} \sim 0.40 - 0.64$ GeV the coupling

strength takes a value around $g_{\sigma\pi\pi} \sim 1.932 - 2.611$ GeV.
Within [62] a finite temperature analysis of the triangle for a similar truncation has also been presented, which, in the limit $T \to 0$ yields the following results for the mass, the decay width and the coupling strength: $M_\sigma = 590$ MeV, $g_{\sigma\pi\pi} = 2.2$ GeV and therefore $\Gamma_{\sigma\to\pi\pi} \simeq 0.22$ GeV.
We postpone the presentation of our own detailed numerical results including simple calculations and the full structure implementation of all concerning BS amplitudes to future publications.

Chapter 5

The $\sigma - \pi\pi - \sigma$ Diamond Diagram, Conclusions and Outlook

In the last chapters we derived and calculated expressions for the quark propagator (c.f. Chap. 2), the Bethe-Salpeter amplitudes for the iso-scalar σ meson and the pseudo-scalar pion case (c.f. Chap. 3) and finally in Chap. 4 these intermediate results were used to construct the decay of the σ into two pions aiming at information about the coupling strength between the three involved particles and the decay width $\Gamma_{\sigma\to\pi\pi}$.
Up to now the σ was considered as a *pure* $q\bar{q}$-state as can be straightforwardly seen reconsidering the calculation in Chap. 3 for the iso-scalar case. Nevertheless the obtained mass lies around 670 MeV and thus differs considerably from other approaches, e.g. [27], that place the σ around 441 MeV. In addition not having considered complex momenta P no information up to now was given about the decay width of the σ.
The goal of this chapter is now to use the obtained pieces of information to construct a diagram contributing to the self-energy $\Pi_\sigma(P^2)$ of the σ meson involving the dominant [2] process of the σ decaying into to pions. As of the, in general, complex nature of $\Pi_\sigma(P^2)$ it is possible to end up with an altered value for the mass of the σ and also an altered decay width (compared to Chap. 4). Intuitively one would expect that the lowest order contribution to the σ-self-energy is a process where the σ emits a pion and reabsorbs it again. However this process is forbidden by parity. Therefore the lowest order diagram including the iso-scalar σ and the π and contributing to the self-energy $\Pi_\sigma(P^2)$ is a diagram of the form of Fig. (5.1). It accounts for the σ decaying into two pions and again recombining into the σ. Such a type of diagram is called "diamond diagram" due to its shape. Further this type of diagram has already been under investigation in different studies concerning problems like e.g. the η'-mass calculation in [12]. In the following section we will construct an expression for the diamond diagram and give insights and suggestions what we expect from its calculation. Further we will give an outlook what has to be done to calculate the

diagram and what is expected to happen to the mass of the σ and its decay width.

5.1 Constructing the Diamond Diagram

Before constructing the diamond we turn briefly back to the expression for the triangle diagram. As it is an ingredient for the diamond it is advantageous to redefine the triangle invariant amplitude $\Gamma_{\sigma\to\pi\pi}$ as a sum over two times the same product of BS amplitudes and quark propagators only with the S_1–quark propagator's momentum altered. This accounts for a possible change of orientation of the internal loop momentum Q. With this changes taken into account the invariant matrix element for the triangle diagram, as depicted in Fig. (4.1), becomes

$$\begin{aligned}\Gamma_{\sigma\to\pi\pi} = N_c \frac{1}{\sqrt{2}} \int_\varepsilon^\Lambda \mathrm{d}^4k \, \Big\{ \mathrm{tr}_D \, \Big[& \Gamma_\sigma(P, k_+^Q) \;\; S_2(k_{-+}^{P,Q}) \times \\ & \times \Gamma_{\pi;3}(P/2 - Q, k - P/4) \;\; S_1(k_-^Q) \times \\ & \times \bar{\Gamma}_{\pi;2}(P/2 + Q, k + P/4) \;\; S_3(k_{++}^{P,Q}) \Big] + \\ + \, \mathrm{tr}_D \, \Big[& \Gamma_\sigma(P, k_+^Q) \;\; S_2(k_{-+}^{P,Q}) \times \\ & \times \Gamma_{\pi;3}(P/2 - Q, k - P/4) \;\; S_1(k_+^Q) \times \\ & \times \bar{\Gamma}_{\pi;2}(P/2 + Q, k + P/4) \;\; S_3(k_{++}^{P,Q}) \Big] \Big\} . \end{aligned} \tag{5.1}$$

Again the color and flavor structure have been already solved and their respective expressions are apparent in Eq. (5.1) as the prefactors N_c and $\frac{1}{\sqrt{2}}$. Further a short notation for the momenta was introduced to obtain a more concise expression. Thereby superscripts "^{P}" and "^{Q}" symbolize the involved momenta besides k and the subscripts "$_+$" and "$_-$" give the related signs with a factor of $\frac{1}{2}$. Two examples how these rules are applied are shown in Eq. (5.2)

$$k_{++}^{P,Q} = k + P/2 + Q/2 \quad \text{and} \quad k_+^Q = k + Q/2. \tag{5.2}$$

Turning to Fig. (5.1) the self-energy of the σ meson in lowest order impulse approximation is given by the diamond diagram, an 4-dimensional integral in Q, the internal loop momentum, over a product of four terms. The already calculated triangle contributes twice, one time as already calculated in Sec. 4.3 and another time as the complex conjugated expression. As missing connections between the triangle amplitudes we put an expression that accounts for the wanted intermediate pole structure. A suitable form is given by the propagator of a "*bare*", bosonic and massive particle which is denoted by $D_\pi(p)$. These

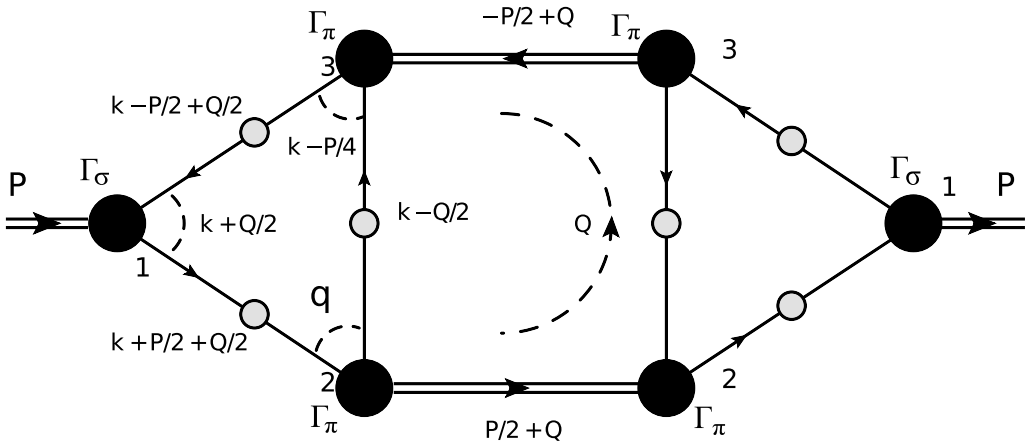

Figure 5.1: The diamond diagram as appearing in the impulse approximation: Double and straight lines denote mesons (σ, π) and quarks respectively. The dashed bows account for the involved relative momenta in the triangle and the loop momentum in the diamond. Further black filled circles denote BS amplitudes whereas grey filled circles denote fully dressed quarks.

stem from the general idea that the quark triangles should be connected by two 4-point Green's functions, each connecting two internal quarks on each side with again two on the other. But as we want to emphasize especially the case of the pions contributing to the σ–self-energy a pole *ansatz*, as in the BSE, is applied to the 4-point Green's functions leading again to a term of the form $\frac{\Gamma\,\bar{\Gamma}}{P^2+M_i^2}$. Having included the amplitudes Γ and $\bar{\Gamma}$ already in the expression(s) for the triangle we are left only to add the denominator terms $D_M(p) := \frac{1}{P^2+M_i^2}$. The self-energy of the σ thus is given in Eq. (5.4)) with the "*bare* pion propagators" involved given by the expression in Eq. (5.3)

$$D_M(p) = \frac{1}{p^2 + M_M^2}, \tag{5.3}$$

$$\Pi(P^2) = \mathrm{tr}_{Dfc} \int \bar{d}^4Q\ \Gamma_{\sigma\to\pi\pi}(P^2, Q^2, P\cdot Q)\ D_\pi(P/2+Q)\ D_\pi(P/2-Q)\ \bar{\Gamma}_{\sigma\to\pi\pi}(P^2, Q^2, -P\cdot Q). \tag{5.4}$$

To solve now for $\Pi(P^2)$ it is straightforward to plug in the associated expressions of the triangles as functions of the two momenta P and Q and solve the four dimensional integral

in Q. However solving this integral entails the necessity to investigate its particular analytic structure as it is needed at points including pole contributions from the pion propagators. Nevertheless a principle value calculation gives a first estimate on the sign of the shift ΔP^2 of the real part of P_σ^2. Moreover considering in general a full calculation of the diamond correction it is not likely that the imaginary shift which contributes to the width Γ will be identical to the one calculated in the "triangle diagram" $\Gamma_{\sigma\to\pi\pi}$. They may however be compatible. Obtaining numerical results is however a still ongoing task and thus beyond the scope of this work. Therefore we conclude with a qualitative discussion of the process shifting the presentation of numerical results to future publications.

5.2 Outlook and Concluding Remarks

In this thesis we gave explicit expressions for the quark Dyson-Schwinger equation and its solution, the quark propagator in Landau gauge. We showed results for both involved dressing functions for two different types of effective interactions. We also considered briefly the needed case in the complex plane. Further the Bethe-Salpeter equation was derived and explicitly applied to the cases of the iso-scalar $q\bar{q}$ σ and the pseudo-scalar pion. In analogy to other calculations [19] we constructed the invariant matrix element for the σ-decay into two pions which is the dominating decay of the $f_0(500)$. We discussed elsewhere obtained results. Finally we gave an expression for the lowest order diagram of the σ–self-energy in impulse approximation to investigate the behavior of the mass and the width of the iso-scalar $q\bar{q}$ state. From the PDG [28] the $f_0(500)$ is known to have a mass between 400 and 550 MeV and a width of 400 to 700 MeV. We arrive at mass of about 660 MeV and expect that in our ongoing calculations the mass of the bare $q\bar{q}$ σ-meson will decrease, due to the contributions from the diamond diagram. Further we described the decay of this iso-scalar state into two pseudo-scalar pions introducing a coupling strength $g_{\sigma\pi\pi}$ and a decay width $\Gamma_{\sigma\to\pi\pi}$. In this context and also via a fully calculated diamond correction we expect extractable information on the width of the particle.

Acknowledgement

In the next lines I would like to thank a few people who contributed to this thesis in one way or another.

First I would like to thank my advisor Dr. Reinhard Alkofer for introducing me into the subject, supporting me wherever it was possible and inspiring me to work in this interesting field, which motivated me every day once again.

I also would like to thank Dr. Richard Williams for his continuous support, the discussions along the way and his patience with me. Furthermore I'm thankful to Dr. Helios Sanchis-Alepuz, who always had time for my newbie questions, whenever they arose, and Dr. Andreas Krassnigg for encouraging working hours from eight o'clock in the morning.

I'm very indebted as well to Karin Dissauer, who encouraged me through her constant questioning about physics and who took apart every line twice, that I wrote, and also Christian Kohlfürst, who joined in swearing with me every time when we were struggling with our PCs.

Next I would like to thank all PhD students of the Doktoratskollegg "Hadrons in Vacuum, Nuclei and Stars", in particular Valentin Mader, Tina Herbst and Andreas Windisch, as well as my colleagues in "Zeitschriftenzimmer" for their time discussing physics and supporting me with coffee whenever physics did have won "the game" against sleep the night before.

Thanks to all my friends, who endured patiently my absence on multiple occasions, because I wanted to do physics, and to be there for me whenever I needed personal motivation or distraction.

Finally I want to thank my family, in particular my brother Stefan, who always supported me in my decisions, helped me wherever it was possible, encouraged me and showed me that hard work always leads to a favorable issue.

Appendix A

Technical Details

A.1 Euclidean Space-Time

In Chap. 1 we stated briefly that we will work in Euclidean spacetime but not how to obtain the transition between it and the commonly known Minkowski spacetime. In this appendix, starting from usually taken Minkowski coordinates we will derive Euclidean coordinates that will simplify dealing with the metric as well as the calculation of integrals. Further we will also give expressions for known quantities of the Clifford algebra as well as an integral measure. We start with a 4-vector in Minkowski spacetime, defined via the first expression in Eq. (A.1),

$$x_\mu^M = \begin{pmatrix} x_0 \\ \vec{x} \end{pmatrix} = (x_0, x_1, x_2, x_3)^T, \qquad \text{and} \qquad g^{\mu\nu} = \eta^{\mu\nu} = \begin{pmatrix} 1 & & & \\ & -1 & & \\ & & -1 & \\ & & & -1 \end{pmatrix}, \quad \text{(A.1)}$$

including the definition of the metric tensor $g^{\mu\nu}$ given in the second part of the equation. The scalar product between two vectors in Minkowski space is further represented by

$$\left(x_\mu^M\right)^2 = \eta^{\mu\nu}\, x_\mu^M\, x_\nu^M = \eta_{\mu\nu}\, x^{\mu;M}\, x^{\nu;M} = x_0^2 - \vec{x}^2 = x_0^2 - x_i^2. \quad \text{(A.2)}$$

Through a Wick rotation in the complex plane of the time-component $x_0 \to -ix_4$ it is possible to map the (3+1)d Minkowski spacetime to a 4d Euclidean spacetime with the definition of a general 4-vector now given by

$$x_\mu^E = \begin{pmatrix} \vec{x} \\ ix_0 =: x_4 \end{pmatrix}, \qquad \text{and} \qquad g^{\mu\nu} = \delta_{\mu\nu} = \begin{pmatrix} 1 & & & \\ & 1 & & \\ & & 1 & \\ & & & 1 \end{pmatrix}, \quad \text{(A.3)}$$

and the metric tensor simplified to the unit matrix $\delta_{\mu\nu}$. Again constructing a scalar product, this time including the new metric tensor, one arrives at the following slightly simpler expression for the scalar product between two, in this case, identical 4-vectors in Euclidean spacetime. It should be stressed that the square of a vector in Euclidean space catches a relative minus sign compared to the Minkowski space

$$\left(x_\mu^E\right)^2 = \delta_{\mu\nu}\, x_\mu^E\, x_\nu^E = \sum_{a=1}^{4} x_a^2 = x_i^2 - x_0^2 = -\left(x_\mu^M\right)^2 . \tag{A.4}$$

Furthermore, these relations can be used to extract information on the transformation properties of 4-dimensional integrals which were often used throughout this thesis. It is straightforward to calculate that the integral over coordinate space catches a factor $-i$ whereas the momentum integral only takes up a factor i:

$$\int_{-\infty}^{\infty} d^4x^M = -i \int_{-\infty}^{\infty} d^4x^E, \tag{A.5}$$

$$\int_{-\infty}^{\infty} d^4k^M = i \int_{-\infty}^{\infty} d^4k^E. \tag{A.6}$$

The idea can be further applied to different structures of 4-vectors but in particular we want to discuss here the changes in Clifford algebra and thus the effect of Euclidean spacetime on gamma matrices. In Minkowski space the Dirac matrices fulfill the Clifford algebra and thus the anti-commutator relation (Eq. (A.7)). Through the requirement that the gamma matrices in Euclidean space should fulfill the same algebra we end up with an anti-commutator relation for the Euclidean gamma matrices. Thus the definitions of the gamma matrices in Euclidean spacetime can be seen in Eq. (A.9)

$$\left\{\gamma^{\mu;M}, \gamma^{\nu;M}\right\} = 2g^{\mu\nu}, \tag{A.7}$$

$$\left\{\gamma_\mu^E, \gamma_\nu^E\right\} = 2\delta_{\mu\nu}, \tag{A.8}$$

$$\gamma_4^E = \gamma_0^M, \tag{A.9}$$

$$\gamma_i^E = -i\gamma_i^M. \tag{A.10}$$

In analogy to the case in Minkowski space (A.11) it is moreover possible to define a quantity γ_5 that commutes with all other newly defined γ^Es which is called again γ_5^E but with a superscript ^{E} indicating the different metric

$$\gamma_5^M = i\gamma_0\gamma_1\gamma_2\gamma_3 = \begin{pmatrix} 0 & \mathbb{1} \\ \mathbb{1} & 0 \end{pmatrix}, \tag{A.11}$$

$$\gamma_5^E := -\gamma_1^E\gamma_2^E\gamma_3^E\gamma_4^E = \begin{pmatrix} 0 & \mathbb{1} \\ \mathbb{1} & 0 \end{pmatrix}. \tag{A.12}$$

In addition the standard representation of the gamma matrices in Euclidean spacetime is briefly given through the expressions in Eq. (A.13). It is now possible to calculate the Feynman slash (also known as the slash product) of a 4-coordinate x^M and a 4-momentum k^M. For simplicity we only state here one of both calculations, i.e. the one for the 4-coordinate x^M, which is given in Eq. (A.14). The Minkowski Feynman slash thereby amounts to minus i times the Euclidean Feynman slash,

$$\gamma_i^E = \begin{pmatrix} 0 & -i\sigma_i \\ i\sigma_i & 0 \end{pmatrix}, \qquad \gamma_4^E = \begin{pmatrix} \mathbb{1} & 0 \\ 0 & -\mathbb{1} \end{pmatrix}, \tag{A.13}$$

$$\not{x}^M = x_0^M \gamma_0^M - x_i^M \gamma_i^M = -i x_4^E \gamma_4^E - x_i^E (i\gamma_i^E) = -i \sum_{i=1}^{4} x_i^E \gamma_i^E = -i \not{x}^E. \tag{A.14}$$

With all expressions in mind we turn to the derivations in chapters one to four where we would like to emphasize two changes due to the transistion from Minkowski to Euclidean metric. The first one is the change in the "on-shell" condition (Eq. (A.15)) where the total momentum squared in Euclidean spacetime becomes "minus" the mass squared and thus the total momentum becomes imaginary. This also plays a crucial role where the quark propagator has to be calculated in the complex plane when it is used as input in the Bethe-Salpeter equation

$$(P_\mu^M)^2 = M^2 \overset{Wick\ rot.}{\Longrightarrow} (P_\mu^E)^2 = -M^2. \tag{A.15}$$

Further, when dealing with Euclidean coordinates it is simple to transform to spherical coordinates (Eq. (A.17)), introducing the absolute value $\sqrt{x^{E;2}}$ and three angles α, θ and ϕ. Through a second transformation of α and θ

$$x_\mu^E = \begin{pmatrix} x_1 \\ x_2 \\ x_3 \\ x_4 \end{pmatrix} \longrightarrow \sqrt{x^2} \begin{pmatrix} \sin(\alpha)\sin(\theta)\sin(\phi) \\ \sin(\alpha)\sin(\theta)\cos(\phi) \\ \sin(\alpha)\cos(\theta) \\ \cos\alpha \end{pmatrix} = \sqrt{x^2} \begin{pmatrix} \sqrt{1-z^2}\sqrt{1-y^2}\sin(\phi) \\ \sqrt{1-z^2}\sqrt{1-y^2}\cos(\phi) \\ \sqrt{1-z^2}y \\ z \end{pmatrix}, \tag{A.16}$$

using the definitions $z := \cos(\alpha)$ and $y := \cos(\theta)$ it is possible to rewrite the 4-vector once again in terms of $\sqrt{x^2}$, z, y and ϕ. This result can be used straightforwardly to rewrite the 4d integral over dx^4 in terms of these newly obtained variables

$$\int_{-\infty}^{\infty} dx^4 = \int_{-\infty}^{\infty} dx_1\, dx_2\, dx_3\, dx_4 = \int_0^{\infty} k^3\, dk \int_0^{2\pi} d\phi \int_0^{\pi} \sin(\alpha)^2\, d\alpha \int_0^{\pi} \sin(\theta)\, d\theta, \tag{A.17}$$

$$\int \frac{dx^4}{(2\pi^4)} \longrightarrow \frac{1}{(2\pi^4)} \int_0^{\infty} dx^2\, \frac{x^2}{2} \int_{-1}^{1} dz \sqrt{1-z^2} \int_{-1}^{1} dy \int_{-\pi}^{\pi} d\phi. \tag{A.18}$$

A.2 Constructing a covariant basis

In this appendix we want to give some details of how the Bethe-Salpeter amplitudes are constructed. In particular we expected in Eq. (3.29) that the BS amplitudes could be decomposed into Dirac/Lorentz, flavor and color structure. All three of them depend on the quantum numbers of the particle under consideration and thus have to be adapted if different particles are considered. In this section we will restrict our description to the two cases of iso-scalar and pseudo-scalar particles with quantum numbers $J^{PC} = 0^{++}$ and 0^{-+}. How to obtain the flavor and color structure for the Bethe-Salpeter amplitude we shift once again to appendix (A.4). We are left over with only Dirac/Lorentz structure and thus can simplify the amplitude of Eq. (3.29) to

$$\Gamma_M(P,q) = \sum_i \mathscr{F}_{i;M}(P^2, q^2, q\cdot P)\ \tau_{i;M}(P,q). \tag{A.19}$$

As can be seen in Eq. (A.19) it is possible to span the Bethe-Salpeter amplitude in Dirac space onto a basis with basis elements $\tau_{i;M}$ and coefficients $\mathscr{F}_{i;M}$. The basis elements depend on the same momenta as the general amplitude whereas the coefficients solely depend on the squares of the related momenta. Moreover to investigate orthogonality and linear independence we define the scalar product between two basis-elements to be given by the trace of their product

$$\langle \tau_i | \tau_j \rangle = \mathrm{tr}(\tau^i \cdot \tau^j) = \delta^{ij}. \tag{A.20}$$

Having clarified how to obtain linearly independent elements we turn now to the particular case of an iso-scalar meson and construct its basis in Dirac space. As we want to get a basis for a scalar particle we suspect to obtain scalar basis elements. As is visible in Eq. (A.19) the Bethe-Salpeter amplitude depends on three different quantities which we will use to construct a basis, i.e. P^μ, q^μ and γ^μ. Scalar products between the single 4-vectors can be constructed in six ways. However three of them are proportional to the unit element $\mathbb{1}$ and two of them give 0. Thus we are tempted to take the unity ($\mathbb{1}$) as a first basis element and because P and q are orthogonal to the unit element we can also choose one of them to be the second basis element. Nevertheless as Eq. (A.21f) is non-vanishing, obviously P and q are not orthogonal. This can be corrected through a Gram-Schmidt procedure step and leads to Eq. (A.22) substracting the non-orthogonal part from the vector q leaving three

orthogonal basis vectors $\mathbb{1}$, P and $q^T = q - P\frac{q.P}{P^2}$

$$\mathrm{tr}(\mathbb{1}\cdot\mathbb{1}) = \mathbb{1}, \tag{A.21a}$$
$$\mathrm{tr}(\mathbb{1}\cdot\not{P}) = 0, \tag{A.21b}$$
$$\mathrm{tr}(\mathbb{1}\cdot\not{q}) = 0, \tag{A.21c}$$
$$\mathrm{tr}(\not{P}\cdot\not{P}) = 4P^2\cdot\mathbb{1}, \tag{A.21d}$$
$$\mathrm{tr}(\not{q}\cdot\not{q}) = 4q^2\cdot\mathbb{1}, \tag{A.21e}$$
$$\mathrm{tr}(\not{P}\cdot\not{q}) = 4q.P, \tag{A.21f}$$

$$q \Longrightarrow q - P\frac{q.P}{P^2}. \tag{A.22}$$

To check if the two newly chosen basis elements are really orthogonal one again applies the trace and indeed obtains zero for the traced product between P and q^T

$$\mathrm{tr}(\not{P}\cdot(\not{q} - \not{P}\frac{q.P}{P^2})) = 0. \tag{A.23}$$

Having found three linear independent basis elements it is still necessary to check if there could be more basis elements. In the case of the iso-scalar state it is possible by considering scalar products of already obtained scalar products, e.g. $\not{q}\not{P}$, to find a fourth basis element given by the commutator of the scalar product $i\,[\not{q},\not{P}]$. Checking out of convenience also the other possible scalar products gives nothing new since Eqs. (A.24a) - (A.24b) are both proportional to the unit element and scalar products of more terms also just reproduce the dependence on the mentioned four elements

$$\not{q}\not{q} = q^2\cdot\mathbb{1}, \tag{A.24a}$$
$$\not{P}\not{P} = P^2\cdot\mathbb{1}. \tag{A.24b}$$

In addition we also list them in Table A.1 For the pseudo-scalar case we remember the fact that the γ_5 matrix is negative under parity and thus we obtain basis elements for the pseudo-scalar meson states by multiplying the obtained basis by a factor of γ_5. Finally the orthonormalised basis elements for the iso-scalar and the pseudo-scalar $q\bar{q}$ state are given in detail in Table A.1.

We use the obtained basis to construct the Dirac structure of the iso-scalar σ Bethe-Salpeter amplitude with coefficients E, F, G and H (c.f. Eq. (A.25)), which depend as discussed above only on the squared momenta P^2, q^2 and $q\cdot P$. An analogous construction can be made for the pseudo-scalar pion Bethe-Salpeter amplitude $\Gamma_\pi(P,q)$

$$\Gamma_\sigma(P,q) = \Big[E_\sigma(P^2,q^2,q\cdot P)\;\frac{1}{2}\mathbb{1}\;+\;F_\sigma(P^2,q^2,q\cdot P)\;\widehat{\not{P}}\;+\;G_\sigma(P^2,q^2,q\cdot P)\,\widehat{\not{q}^T}\;+ \\ +\;H_\sigma(P^2,q^2,q\cdot P)\;\Big[\widehat{\not{q}},\,\widehat{\not{P}}\Big]\Big]. \tag{A.25}$$

Table A.1: The Lorentz-covariant basis of the Bethe-Salpeter amplitudes

	scalar case: 0^{++}	pseudo-scalar case: 0^{-+}
$\tau_1(P,q)$	$\frac{1}{2}\mathbb{1}$	$\frac{\gamma_5}{2}\,\mathbb{1}$
$\tau_2(P,q)$	$\frac{i}{2\sqrt{-P^2}}\not{P}$	$\frac{i\gamma_5}{2\sqrt{P^2}}\not{P}$
$\tau_3(P,q)$	$\frac{i}{2\sqrt{\frac{(P.q)^2}{P^2}-q^2}}(\not{q}-\not{P}\frac{P.q}{P^2})$	$\frac{i\,\gamma_5}{2\sqrt{q^2\,(P.q)^2-\frac{(P.q)^4}{P^2}}}(\not{q}(P.q)-\not{P}\frac{(P.q)^2}{P^2})$
$\tau_4(P,q)$	$\frac{1}{4}\,\frac{1}{\sqrt{q^2\,P^2-(P.q)^2}}\,\left[(\not{q}-\not{P}\frac{P.q}{P^2})\,,\,\not{P}\right]$	$\frac{1}{4}\,\frac{1}{\sqrt{q^2\,P^2-(P.q)^2}}\,\left[(\not{q}-\not{P}\frac{P.q}{P^2})\,,\,\not{P}\right]$

A.3 Kinematics of the Triangle Diagram

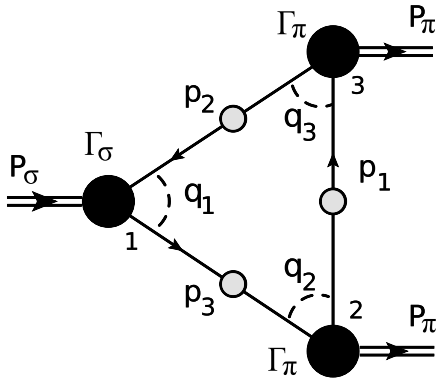

Figure A.1: The triangle diagram: kinematics and involved momenta

In this appendix we want to discuss the kinematics of the triangle diagram introduced in Chap. 4. As input therein quark propagators and Bethe-Salpeter amplitudes were used. Assuming overall energy-momentum conservation, which is also expressed through Eq. (A.26), the momenta contributing in a general consideration of the Bethe-Salpeter equation are the incoming total momentum P_i of the composite particle under consideration, the relative momentum q_i and the outgoing quark (i.e. $q_{i;+}$) and outgoing anti-quark momentum $q_{i;-}$

$$0 = P_\sigma - P_{\pi_2} - P_{\pi_3}. \tag{A.26}$$

Their definitions can be seen in Eq. (A.27)

$$\left.\begin{array}{rcl} P_i &=& q_{i;+} - q_{i;-}, \\ q_i &=& \bar{\eta} q_{i;+} + \eta q_{i;-}, \end{array}\right\} \qquad \begin{array}{l} q_{i;+} = q_i + \eta_i P_i, \\ q_{i;-} = q_i - \bar{\eta}_i P_i. \end{array} \tag{A.27}$$

The variables η and $\bar{\eta}$ account for the momentum partitioning between the two constituent particles of the Bethe-Salpeter equation. They have to be fixed a priori before the calculation and will depend on the Bethe-Salpeter amplitude under investigation but are in general free to choose between 0 and 1 as they only need to fulfill $\eta + \bar{\eta} = 1$. We have seen in the case of the BSE calculation that the momentum partitioning parameters, however, affect the region in the complex plane where the constituent quark and anti-quarks for the BSE have to be calculated.
If one considers now the triangle diagram it is necessary to take three total momenta, three relative momenta and three quark momenta into account. We therefore introduce the following notation (also already used in [19]): Capital P's will label the total momenta of the BS amplitudes, the q's the relative momenta and the p's will account for the quark momenta needed in the diagram. As can be seen already in (A.26) all BS amplitudes were considered as incoming states. In the context of the triangle diagram this should not affect the calculations, however when the triangle is taken as an input for another diagram the right momentum flow has to be taken into account. Through the definition of the momenta of the quarks contributing to the BSE and the identification of them with the quark propagators it is straightforward to rewrite the quark momenta in terms of the relative momenta as well as the partitioning parameters and the total momenta of the particles. Written in a compactified notation, each internal quark line in the triangle has two restricting equations

$$\left.\begin{array}{rcl} p_1 &=& q_3 - \bar{\eta}_3 P_3, \\ p_2 &=& q_3 - \eta_3 P_3, \\ p_2 &=& q_1 - \bar{\eta}_1 P_1, \\ p_3 &=& q_1 - \eta_1 P_1, \\ p_3 &=& q_2 - \bar{\eta}_2 P_2, \\ p_1 &=& q_2 - \eta_2 P_2. \end{array}\right\} \qquad \begin{array}{l} p_1 : q_3 - \bar{\eta}_3 P_3 = q_2 + \eta_2 P_2 \\ p_2 : q_3 - \eta_3 P_3 = q_1 + \bar{\eta}_1 P_1 \\ p_3 : q_1 - \eta_1 P_1 = q_2 + \bar{\eta}_2 P_2 \end{array} \tag{A.28}$$

Thus we get relations between the relative momenta leading to a re-expression of the relative momenta of the pions, visible in Fig. (A.1). In Eq. (A.29) we give the relative momenta q_2 and q_3 as functions of the relative momentum of the particle at position 1 and all contributing total momenta. Furthermore the quark momenta can also be re-expressed as functions of the same momenta q_1, P_1, P_2 and P_3 and their related partitioning parameters:

$$\begin{array}{rcl} q_3 &=& q_1 - \bar{\eta}_1 P_1 - \eta_3 P_3, \\ q_2 &=& q_1 - \eta_1 P_1 + \bar{\eta}_2 P_2. \end{array} \tag{A.29}$$

Further, as the triangle is considered in the iso-symmetric case with equal-mass constituent quarks, it is convenient to choose the momentum partitioning of the BSE at point 1 symmetrically to $\frac{1}{2}$. If considering in particular the iso-scalar σ decaying into two pions point

1 will also be identified as the decaying iso-scalar BS amplitude

$$\eta_1 = \eta_\sigma = \frac{1}{2} = \bar{\eta}_\sigma = \bar{\eta}_1, \tag{A.30}$$

which leaves us just with four unknown momentum partitioning η's besides the four momenta with which we expressed all others.
If one wants now to study a certain process via a practical calculation it is necessary to select a certain frame of reference. Two choices are the well-known Breit-frame or the rest-frame of the decaying particle. For the purpose of this work we will stick to a frame in which the σ is at rest and thus the total momentum of the iso-scalar σ becomes most simplest (c.f. Eq. (A.31)). Nevertheless the calculation must, of course, be independent of the chosen frame. Thus considering the particular triangle diagram of the iso-scalar σ decaying into two pions we identify point 1 in Fig. (A.1) as the σ and the points 2 and 3 as the pions. Moreover the relative momentum of the iso-scalar particle will just be given by q_1 whereas the pion-related momenta are adjusted to account for outgoing pseudo-scalar particles, i.e. they pick up a factor of (-1). The total momenta P_2 and P_3 also change sign

$$\begin{aligned} P_\sigma \quad &:= \quad P_1 \quad \overset{\text{at rest}}{=} \begin{pmatrix} 0 \\ 0 \\ 0 \\ iM_\sigma \end{pmatrix} \quad ; \qquad q_\sigma \quad := \quad q_1 \\ P_{\pi_2,\pi_3} \quad &:= \quad -P_{2,3} \qquad\qquad\qquad ; \qquad q_{\pi_2,\pi_3} \quad := \quad -q_{2,3}. \end{aligned} \tag{A.31}$$

Having now obtained expressions for all momenta appearing in the triangle diagram it is advantageous to seek a smaller set to calculate the process. Fixing the total momentum of the decaying σ as a first variable, it is possible to choose the partition of momentum flow between the final pion states symmetrically and we can write the total momenta of the pions at points 2 and 3 as

$$P_\sigma = P; \qquad P_{\pi_2} = \begin{pmatrix} 0 \\ 0 \\ \kappa \\ i\sqrt{M_\pi^2 + \kappa^2} \end{pmatrix}, \qquad P_{\pi_3} = \begin{pmatrix} 0 \\ 0 \\ -\kappa \\ i\sqrt{M_\pi^2 + \kappa^2} \end{pmatrix}. \tag{A.32}$$

The difference between them then yields the definition of a new variable

$$Q := \frac{1}{2}\left(P_{\pi_2} - P_{\pi_3}\right) = \begin{pmatrix} 0 \\ 0 \\ \kappa \\ 0 \end{pmatrix}, \tag{A.33}$$

with κ being defined as a momentum partitioning between the pion momenta contributing

$$\kappa = \sqrt{\frac{M_\sigma^2}{4} - M_\pi^2}. \tag{A.34}$$

With this new momentum variable Q the total momenta of the pions also can be rewritten in terms of only these two newly incorporated variables, i.e. the "incoming" momentum P and the "relative" momentum between the "outgoing" particles Q. The first is given through the σ whereas the latter is obtained via the entity κ linking the masses of the decaying iso-scalar and the resulting pseudo-scalar particle states together

$$P_{\pi_2} = \frac{1}{2}P + Q, \qquad P_{\pi_3} = \frac{1}{2}P - Q. \tag{A.35}$$

Applying the same procedure to the relative momenta of the Bethe-Salpeter amplitudes their expressions yield dependencies on three, already mentioned, momentum variables:

$$q_1 = q_\sigma, \tag{A.36}$$

$$q_2 = -q_{\pi_2} = q_\sigma + \frac{1}{2}P - \bar{\eta}_2\left(\frac{1}{2}P + Q\right), \tag{A.37}$$

$$q_3 = -q_{\pi_3} = q_\sigma - \frac{1}{2}P + \eta_2\left(\frac{1}{2}P - Q\right). \tag{A.38}$$

As the triangle is essentially an internal quark loop diagram it is necessary to introduce also a loop momentum for the quark loop which will be integrated over. All our momenta are already expressed via the two external variables P and Q as well as q_σ. As we want to decrease moreover the region in the complex plane where the Bethe-Salpeter amplitudes have to be known we choose the integration variable as

$$k := q_\sigma - \frac{1}{2}Q. \tag{A.39}$$

Due to iso-symmetric limit we can take also

$$\eta_2 = \bar{\eta}_2 = \frac{1}{2} = \eta_3 = \bar{\eta}_3, \tag{A.40}$$

yielding a short summary of all included momenta as functions of the loop momentum k, the total momentum P and the relative momentum between the pions Q:

$$\boxed{q_\sigma = k + \frac{1}{2}Q,} \tag{A.41}$$

$$\boxed{-q_{\pi_2} = \ldots = k + \frac{1}{4}P,} \tag{A.42}$$

$$\boxed{-q_{\pi_3} = \ldots = k - \frac{1}{4}P,} \tag{A.43}$$

$$\boxed{\begin{aligned} p_1 &= \ldots = k - \frac{1}{2}Q, && \text{(A.44)}\\ p_2 &= \ldots = k - \frac{1}{2}P + \frac{1}{2}Q, && \text{(A.45)}\\ p_3 &= \ldots = k + \frac{1}{2}P + \frac{1}{2}Q, && \text{(A.46)} \end{aligned}}$$

$$\boxed{\begin{aligned} P_1 &= P_\sigma = P, && \text{(A.47)}\\ P_{\pi_2} &= \frac{1}{2}P + Q, && \text{(A.48)}\\ P_{\pi_3} &= \frac{1}{2}P - Q. && \text{(A.49)} \end{aligned}}$$

We leave out the final step of considering the squares of this expressions as they are also needed in the Lorentz-invariant coefficient functions of the Bethe-Salpeter amplitudes as well as the quark dressing functions.

A.4 The flavor and color Structure of the Triangle Diagram

In appendix A.2 we discussed the construction of the Bethe-Salpeter amplitudes concerning the Dirac/Lorentz structure but omitted the flavor and color degrees of freedom. In this section we want now to catch up and describe the included flavor and color structures which will also be needed as input for the construction of the triangle diagram. We will first construct flavor matrices using group theoretical properties then discuss the case of color.

A.4.1 Flavor

We deal with only two flavors of quarks, i.e. up and down, in the iso-symmetric limit where both share the same mass. These two form a doublet $(u\ d)^T$ under transformations with respect to the group SU(2). The quarks thereby transform in the so-called fundamental representation, denoted by 2, whereas the anti-quarks transform in the complex-conjugated fundamental representation $\bar{2}$. In the further scope of this section we will give transformation properties and finally arrive at the generators of the underlying symmetry group. Further on, in the case of mesons we need to combine a quark and an anti-quark via the combination of the two representations (2 and $\bar{2}$)

$$SU(2) \otimes SU(2): \qquad 2 \otimes \bar{2} = 1_a \oplus 3_s, \tag{A.50}$$

with 1_a being an antisymmetric iso-singlet state and 3_s a symmetric iso-triplet state resulting from group theoretical considerations.
The up- and down-quark each have isospin $\frac{1}{2}$ and isospin projection $+\frac{1}{2}$ and $-\frac{1}{2}$ respectively. Analogously to common quantum mechanics it is possible to derive matrix representations for the isospin-projection operators $\tau_{1;2;3}$ and construct with them ladder operators τ_+ and τ_- to raise and low the isospin as it is equivalently done in the theory of angular momentum, e.g. [64]. For convenience we state the isospin projection of u, i.e. $\tau_3 u$ is equal to $\frac{1}{2}$ and the respective expression for d gives $\tau_3 d = -\frac{1}{2}$. The ladder operators then raise and lower the isospin accordingly, i.e. e.g. $\tau_+ d = u$. With this properties in mind we can deduce the matrix representations of the τ_i's which look like

$$\tau_1 = \frac{1}{2}\begin{pmatrix} 0 & 1 \\ 1 & 0 \end{pmatrix} = \frac{\sigma_1}{2}, \quad \tau_2 = \frac{1}{2}\begin{pmatrix} 0 & -i \\ i & 0 \end{pmatrix} = \frac{\sigma_2}{2}, \quad \tau_3 = \frac{1}{2}\begin{pmatrix} 1 & 0 \\ 0 & -1 \end{pmatrix} = \frac{\sigma_3}{2}, \tag{A.51}$$

$$\tau_+ = \begin{pmatrix} 0 & 1 \\ 0 & 0 \end{pmatrix}, \quad \tau_- = \begin{pmatrix} 0 & 0 \\ 1 & 0 \end{pmatrix}. \tag{A.52}$$

In the same manner it is possible to get information on the complex conjugate fundamental representation. There, one can either postulate the complex conjugate representation $\bar{2}$ or derive the matrix representations for the respective isospin projection and ladder operators accordingly in comparison to the fundamental representation of the quarks. How this is done can be seen in standard literature on quantum mechanics (e.g. [64]) and therefore is skipped here for the sake of brevity. We just state again the resulting matrix representation for the projectors and ladder operators $\bar{\tau}_i$. If the complex conjugate fundamental representation is postulated the resulting generators are connected to the already obtained fundamental representation for the quarks via

$$\bar{\tau}_i = -\tau_i^*. \tag{A.53}$$

The ladder operators can then evaluated to be

$$\bar{\tau}_+ = \begin{pmatrix} 0 & 0 \\ -1 & 0 \end{pmatrix}, \quad \bar{\tau}_- = \begin{pmatrix} 0 & -1 \\ 0 & 0 \end{pmatrix}. \tag{A.54}$$

To construct now meson states out of the mentioned product space $SU(2) \otimes SU(2)$ it is necessary to reconsider the example theory of angular momentum. There eigenstates of the rotation operator are classified by the quadratic Casimir operator, J^2, and the 3-axis projection, J_3, in a unique way. The Casimir in the case of $SU(2)$ is given by

$$\sum_i \tau_i^2 = \sum_i \bar{\tau}_i^2 = \frac{3}{4}\mathbb{1} \tag{A.55}$$

which is related to a total isospin of $\frac{1}{2}$. To specify now an irreducible representation of the product group $SU(2) \otimes SU(2)$ the use of Clebsch-Gordon coefficients is needed. We

therefore express a composite state in isospin space in analogy with the case of angular momentum and case of the spin-$\frac{1}{2}$ electron in quantum mechanics as

$$|j,m\rangle = \sum_{m_1,m_2} |j_1,m_1;j_2,m_2\rangle \langle j_1,m_1;j_2,m_2|j,m\rangle, \tag{A.56}$$

whereas j was the total angular momentum or spin of the composite state, m its projection onto the 3-axis and the analogous variables for the single momentum/spin states $j_{1;2}$ and $m_{1;2}$. Following the treatment of angular momentum one fixes a particular j, in the considered case of two quark flavors this ammounts to $\frac{1}{2}$, chooses the maximal (or minimal) related projection $m_{\max}(j)$ and applies one of the two composite ladder operators $T_-^{2\otimes\bar{2}}$ or $T_+^{2\otimes\bar{2}}$ to obtain all other $m(j)$s. The lowering ladder operator needed to construct all composite states in the case of angular momentum theory is given in Eq. (A.57)

$$J_-|j,m\rangle = \sqrt{(j+m)\,(j-m+1)}|j,m-1\rangle. \tag{A.57}$$

In the case of the combined isospin symmetry to create mesons as quark–anti-quark bound states the lowering ladder operator is given through the direct sum of obtained ladder operators in isospin space

$$T_-^{2\otimes\bar{2}} = \tau_- \oplus \bar{\tau}_-. \tag{A.58}$$

To evaluate now the resulting states in the product space it is advantageous to choose a suitable basis. As was stated in the beginning the u- and d-quarks form a doublet, thus, applying the outer product of the product space, gives a 2×2 matrix. A suitable basis for hermitian 2×2 matrices is given by the Pauli matrices σ_i and the unit matrix $\mathbb{1}$. We therefore span the outer products in this basis obtaining e.g. for the isospin $\tau = 1$, $\tau_3 = 1$ case

$$|u\bar{d}\rangle = \begin{pmatrix}1\\0\end{pmatrix} \otimes \begin{pmatrix}0\\1\end{pmatrix} = \begin{pmatrix}0 & 1\\0 & 0\end{pmatrix} = \frac{1}{2}\left(\sigma_1 + i\sigma_2\right), \tag{A.59}$$

which corresponds, as written down already, to the $u\bar{d}$ mesonic state. Applying now the mentioned ladder operator in the product space yields all other $\tau = 1$ states, listed as follows

$$\mathbb{s}^+ = |u\bar{d}\rangle = \frac{1}{2}\left(\sigma_1 + i\sigma_2\right), \tag{A.60}$$

$$\mathbb{s}^0 = \frac{1}{\sqrt{2}}\left(|d\bar{d}\rangle - |u\bar{u}\rangle\right) = -\frac{1}{\sqrt{2}}\sigma_3, \tag{A.61}$$

$$\mathbb{s}^- = -|d\bar{u}\rangle = -\frac{1}{2}\left(\sigma_1 - i\sigma_2\right), \tag{A.62}$$

$$\mathbb{s}^s = \frac{1}{\sqrt{2}}\left(|d\bar{d}\rangle + |u\bar{u}\rangle\right) = \frac{1}{\sqrt{2}}\,\mathbb{1}_f. \tag{A.63}$$

Using now these results for the flavor structure of the Bethe-Salpeter amplitudes it is possible to construct the flavor trace for the triangle diagram. Thereby the iso-scalar meson is given via the singlet state in flavor space whereas the pseudo-scalar mesons are known to be an iso-triplet and thus incorporate one of the three triplet flavor structures ${}_{\mathbb{S}}{}^{+;0;-}$.

A.4.2 Color

Analogously to the case of flavor it is possible to investigate the case of color. As well as in the previous section the quarks transform according to the fundamental representation of the underlying symmetry group. In the case of color, however, the construction of singlets, triplets, octets, etc. is drastically simplified by the fact that hadrons are color singlets. Thus it is only necessary to construct an antisymmetric color singlet state. In direct comparison to Eq. (A.63) color singlets are constructed out of the fundamental representation accounting for the quarks and the complex-conjugated fundamental representation dealing with the anti-quarks

$$SU(3) \otimes SU(3): \qquad 3 \otimes \bar{3} = 1_a \oplus 8_s. \tag{A.64}$$

In analogy to Eq. (A.63) the color singlet case can be constructed with r,b and g the color degrees of freedom red, green and blue. Further for two arbitrary colors the unit element is expressed through a δ-functional in color space

$$\mathbb{c}^s = \frac{1}{\sqrt{3}} \left(|r\bar{r}\rangle + |g\bar{g}\rangle + |b\bar{b}\rangle \right) = \frac{1}{\sqrt{3}} \, \mathbb{1}_C = \frac{1}{\sqrt{3}} \, \delta_{A\bar{B}}. \tag{A.65}$$

Bibliography

[1] C. Itzykson and J. Zuber, *Quantum Field Theory.* 1980.

[2] K. Nakamura *et al.*, "Review of particle physics," *J.Phys.G*, vol. G37, p. 075021, 2010.

[3] M. E. Peskin and D. V. Schroeder, *An Introduction to quantum field theory.* 1995.

[4] L. Ryder, *Quantum Field Theory.* 1985.

[5] S. Weinberg, *The quantum theory of fields. Vol. 2: Modern applications.* 1996.

[6] T. Muta, *Foundations of quantum chromodynamics: An Introduction to perturbative methods in gauge theories*, vol. 5. 1987.

[7] L. Faddeev and V. Popov, "Feynman Diagrams for the Yang-Mills Field," *Phys.Lett.*, vol. B25, pp. 29–30, 1967.

[8] C. N. Yang and R. L. Mills, "Conservation of isotopic spin and isotopic gauge invariance," *Phys. Rev.*, vol. 96, pp. 191–195, Oct 1954.

[9] S. L. Adler, "Anomalies in Ward Identities and Current Commutation Relations," 1971.

[10] J. Bell and R. Jackiw, "A PCAC puzzle: pi0 to gamma gamma in the sigma model," *Nuovo Cim.*, vol. A60, pp. 47–61, 1969.

[11] G. 't Hooft, "Symmetry breaking through bell-jackiw anomalies," *Phys. Rev. Lett.*, vol. 37, pp. 8–11, Jul 1976.

[12] R. Alkofer, C. S. Fischer, and R. Williams, "U(A)(1) anomaly and eta-prime mass from an infrared singular quark-gluon vertex," *Eur.Phys.J.*, vol. A38, pp. 53–60, 2008.

[13] R. P. Feynman, *The principle of least action in quantum mechanics.* PhD thesis, 1942.

[14] J. S. Schwinger, "On the Green's functions of quantized fields. 1.," *Proc.Nat.Acad.Sci.*, vol. 37, pp. 452–455, 1951.

[15] J. S. Schwinger, "On the Green's functions of quantized fields. 2.," *Proc.Nat.Acad.Sci.*, vol. 37, pp. 455–459, 1951.

[16] H. Lehmann, K. Symanzik, and W. Zimmermann, "On the formulation of quantized field theories," *Nuovo Cim.*, vol. 1, pp. 205–225, 1955.

[17] F. Dyson, "The Radiation theories of Tomonaga, Schwinger, and Feynman," *Phys.Rev.*, vol. 75, pp. 486–502, 1949.

[18] F. Dyson, "The S matrix in quantum electrodynamics," *Phys.Rev.*, vol. 75, pp. 1736–1755, 1949.

[19] V. Mader, G. Eichmann, M. Blank, and A. Krassnigg, "Hadronic decays of mesons and baryons in the Dyson-Schwinger approach," *Phys.Rev.*, vol. D84, p. 034012, 2011.

[20] J. R. Taylor, *Scattering Theory: The Quantum Theory of Nonrelativistic Collisions.* Dover Books on Engineering, 31 East 2nd Street, Mineola. N.Y. 11501: Dover Publications Inc., dover edition 2006 ed., 2006.

[21] C. Gattringer and C. B. Lang, "Quantum chromodynamics on the lattice," *Lect.Notes Phys.*, vol. 788, pp. 1–211, 2010.

[22] R. Alkofer and L. von Smekal, "The Infrared behavior of QCD Green's functions: Confinement dynamical symmetry breaking, and hadrons as relativistic bound states," *Phys.Rept.*, vol. 353, p. 281, 2001.

[23] G. Wick, "Properties of Bethe-Salpeter Wave Functions," *Phys.Rev.*, vol. 96, pp. 1124–1134, 1954.

[24] R. Rivers, *Path Integral Methods in Quantum Field Theory.* 1987.

[25] Y. Nambu and G. Jona-Lasinio, "Dynamical Model of Elementary Particles Based on an Analogy with Superconductivity. II," *Phys.Rev.*, vol. 124, pp. 246–254, 1961.

[26] Y. Nambu and G. Jona-Lasinio, "Dynamical Model of Elementary Particles Based on an Analogy with Superconductivity. 1.," *Phys.Rev.*, vol. 122, pp. 345–358, 1961.

[27] I. Caprini, G. Colangelo, and H. Leutwyler, "Mass and width of the lowest resonance in QCD," *Phys.Rev.Lett.*, vol. 96, p. 132001, 2006.

[28] J. Beringer *et al.*, "2012 Review of particle physics," *Phys. Rev. D*, vol. D86, p. 010001, 2012.

[29] N. A. Tornqvist and M. Roos, "Resurrection of the sigma meson," *Phys.Rev.Lett.*, vol. 76, pp. 1575–1578, 1996.

[30] S. Roy, "Exact integral equation for pion pion scattering involving only physical region partial waves," *Phys.Lett.*, vol. B36, p. 353, 1971.

[31] J. Pelaez, "On the Nature of light scalar mesons from their large N(c) behavior," *Phys.Rev.Lett.*, vol. 92, p. 102001, 2004.

[32] J. Pelaez, "Light scalars as tetraquarks or two-meson states from large N(c) and unitarized chiral perturbation theory," *Mod.Phys.Lett.*, vol. A19, pp. 2879–2894, 2004.

[33] M. Schumacher, "Structure of scalar mesons and the Higgs sector of strong interaction," *J.Phys.G*, vol. G38, p. 083001, 2011.

[34] R. Garcia-Martin, R. Kaminski, J. Pelaez, J. Ruiz de Elvira, and F. Yndurain, "The Pion-pion scattering amplitude. IV: Improved analysis with once subtracted Roy-like equations up to 1100 MeV," *Phys.Rev.*, vol. D83, p. 074004, 2011.

[35] W. Heupel, G. Eichmann, and C. S. Fischer, "Tetraquark bound states in a Bethe-Salpeter approach," 2012.

[36] C. J. Morningstar and M. J. Peardon, "The Glueball spectrum from an anisotropic lattice study," *Phys.Rev.*, vol. D60, p. 034509, 1999.

[37] V. Crede and C. Meyer, "The Experimental Status of Glueballs," *Prog.Part.Nucl.Phys.*, vol. 63, pp. 74–116, 2009.

[38] G. Grayer, B. Hyams, C. Jones, P. Schlein, P. Weilhammer, *et al.*, "High Statistics Study of the Reaction pi- p gt; pi- pi+ n: Apparatus, Method of Analysis, and General Features of Results at 17-GeV/c," *Nucl.Phys.*, vol. B75, p. 189, 1974.

[39] R. Kaminski, L. Lesniak, and K. Rybicki, "Separation of S wave pseudoscalar and pseudovector amplitudes in pi- p (polarized) gt; pi+ pi- n reaction on polarized target," *Z.Phys.*, vol. C74, pp. 79–91, 1997.

[40] G. Eichmann, *Hadron Properties from QCD Bound-State Equations*. PhD thesis, 2009.

[41] J. C. Ward, "An Identity in Quantum Electrodynamics," *Phys.Rev.*, vol. 78, p. 182, 1950.

[42] Y. Takahashi, "On the generalized Ward identity," *Nuovo Cim.*, vol. 6, p. 371, 1957.

[43] J. S. Ball and T.-W. Chiu, "Analytic Properties of the Vertex Function in Gauge Theories. 1.," *Phys.Rev.*, vol. D22, p. 2542, 1980.

[44] H. Sanchis-Alepuz, R. Alkofer, G. Eichmann, and R. Williams, "Model comparison of Delta and Omega masses in a covariant Faddeev approach," *PoS*, vol. QCD-TNT-II, p. 041, 2011.

[45] G. Eichmann, "The analytic structure of the quark propagator in the covariant Faddeev equation of the nucleon," Master's thesis, 2006.

[46] P. Maris and C. D. Roberts, "Pi- and K meson Bethe-Salpeter amplitudes," *Phys.Rev.*, vol. C56, pp. 3369–3383, 1997.

[47] P. Maris and P. C. Tandy, "Bethe-Salpeter study of vector meson masses and decay constants," *Phys.Rev.*, vol. C60, p. 055214, 1999.

[48] R. Alkofer, P. Watson, and H. Weigel, "Mesons in a Poincare covariant Bethe-Salpeter approach," *Phys.Rev.*, vol. D65, p. 094026, 2002.

[49] M. Blank, *Properties of quarks and mesons in the Dyson-Schwinger/Bethe-Salpeter approach*. PhD thesis, 06 2011.

[50] C. S. Fischer, "Non-perturbative propagators, running coupling and dynamical mass generation in ghost-antighost symmetric gauges in qcd,"

[51] E. Salpeter and H. Bethe, "A Relativistic equation for bound state problems," *Phys.Rev.*, vol. 84, pp. 1232–1242, 1951.

[52] A. Holl, A. Krassnigg, and C. Roberts, "Pseudoscalar meson radial excitations," *Phys.Rev.*, vol. C70, p. 042203, 2004.

[53] P. Maris, C. D. Roberts, and P. C. Tandy, "Pion mass and decay constant," *Phys.Lett.*, vol. B420, pp. 267–273, 1998.

[54] H. Munczek, "Dynamical chiral symmetry breaking, Goldstone's theorem and the consistency of the Schwinger-Dyson and Bethe-Salpeter Equations," *Phys.Rev.*, vol. D52, pp. 4736–4740, 1995.

[55] R. Cutkosky and M. Leon, "Normalization of Bethe-Salpeter Wave Functions and Bootstrap Equations," *Phys.Rev.*, vol. 135, pp. B1445–B1446, 1964.

[56] N. Nakanishi, "Normalization Condition and Normal and Abnormal Solutions of the Bethe-Salpeter Equation," *Phys.Rev.*, vol. 138, pp. B1182–B1192, 1965.

[57] R. Williams, "Bethe-Salpeter studies of mesons beyond rainbow-ladder," 2009.

[58] C. S. Fischer and R. Williams, "Probing the gluon self-interaction in light mesons," *Phys.Rev.Lett.*, vol. 103, p. 122001, 2009.

[59] R. Cutkosky, "Solutions of a Bethe-Salpeter equations," *Phys.Rev.*, vol. 96, pp. 1135–1141, 1954.

[60] D. Jarecke, P. Maris, and P. C. Tandy, "Strong decays of light vector mesons," *Phys.Rev.*, vol. C67, p. 035202, 2003.

[61] S. Mandelstam, "Analytic properties of transition amplitudes in perturbation theory," *Phys. Rev.*, vol. 115, pp. 1741–1751, Sep 1959.

[62] P. Maris, C. D. Roberts, S. Schmidt, and P. Tandy, "T - dependence of pseudoscalar and scalar correlations," *Phys.Rev.*, vol. C63, p. 025202, 2001.

[63] J. Kuipers, T. Ueda, J. Vermaseren, and J. Vollinga, "FORM version 4.0," 2012.

[64] W. Greiner and B. Müller, *Theoretical physics. Vol. 2: Quantum mechanics. Symmetries.* Springer, 1994.

List of Figures